
Personalized Adapter for Large Meteorology Model on Devices: Towards Weather Foundation Models

Shengchao Chen

AAII, School of CS, FEIT
University of Technology Sydney
shengchao.chen.uts@gmail.com

Guodong Long

AAII, School of CS, FEIT
University of Technology Sydney
Guodong.Long@uts.edu.au

Jing Jiang

AAII, School of CS, FEIT
University of Technology Sydney
Jing.Jiang@uts.edu.au

Chengqi Zhang

AAII, School of CS, FEIT
University of Technology Sydney
Chengqi.Zhang@uts.edu.au

Abstract

This paper demonstrates that pre-trained language models (PLMs) are strong foundation models for on-device meteorological variables modeling. We present LM-WEATHER, a generic approach to taming PLMs, that have learned massive sequential knowledge from the universe of natural language databases, to acquire an immediate capability to obtain highly customized models for heterogeneous meteorological data on devices while keeping high efficiency. Concretely, we introduce a lightweight personalized adapter into PLMs and endows it with weather pattern awareness. During communication between clients and the server, low-rank-based transmission is performed to effectively fuse the global knowledge among devices while maintaining high communication efficiency and ensuring privacy. Experiments on real-world dataset show that LM-WEATHER outperforms the state-of-the-art results by a large margin across various tasks (*e.g.*, forecasting and imputation at different scales). We provide extensive and in-depth analyses experiments, which verify that LM-WEATHER can (1) indeed leverage sequential knowledge from natural language to accurately handle meteorological sequence, (2) allows each devices obtain highly customized models under significant heterogeneity, and (3) generalize under data-limited and out-of-distribution (OOD) scenarios.

1 Introduction

Accurately modeling weather variation pattern from large amount of meteorological variables sequences is increasingly vital for providing efficient weather analysis support for disaster warning. Recently, the promise of learning to understand weather pattern from data via deep learning (DL) has led to an ongoing paradigm shift apart from the long-established physics-based methods [1, 2].

Mining potential patterns from meteorological sequences that collected from different regions, including forecasting and imputation, is one of the most important problems in meteorology. Significant progress has been made by several latest time series approaches [1, 3, 4]. These approaches formulate meteorological variable modeling as an end-to-end spatio-temporal learning problem. This overlooks the reality that ground weather devices distributed globally gather vast amounts of data quickly. The sheer volume of data, coupled with limited network capacity, necessitates local processing on the devices, making centralised learning challenging [5]. On-device intelligence enables edge devices to compute independently, offering a primary solution to the problem.

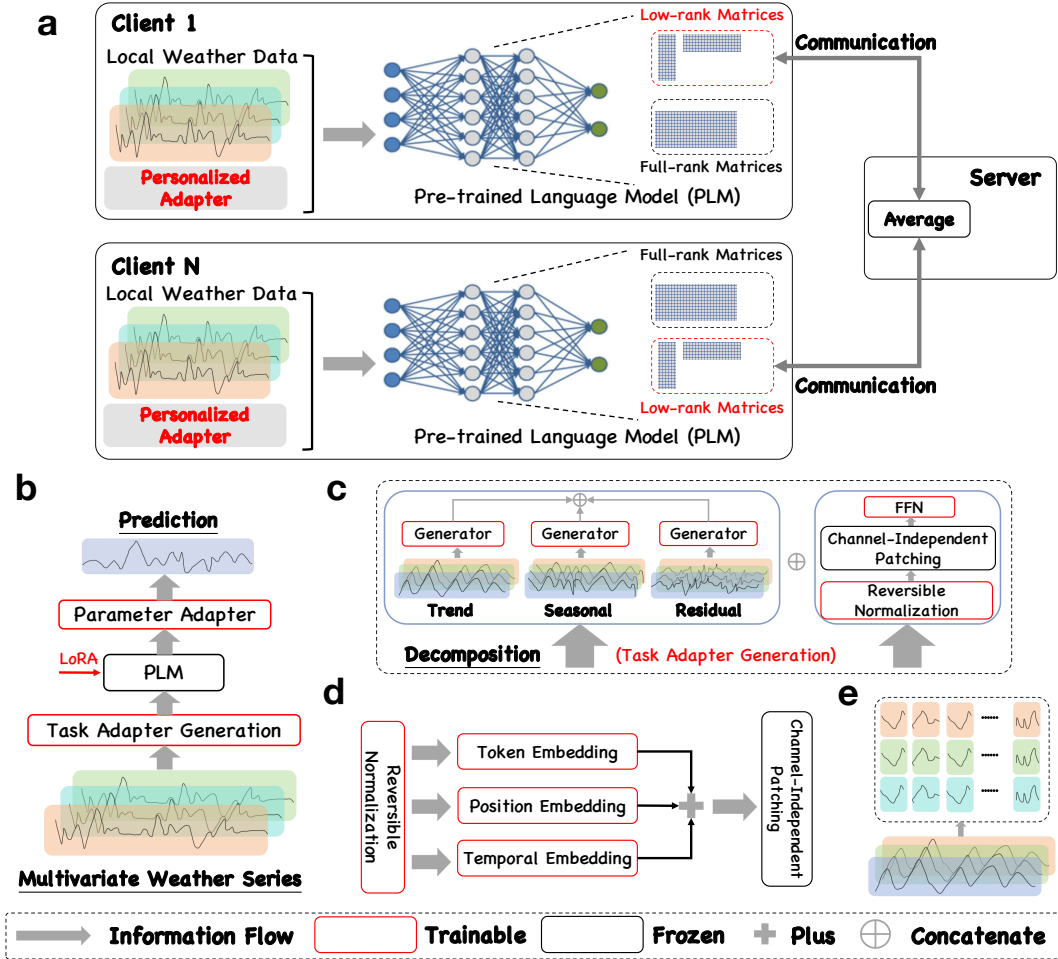


Figure 1: *Overview*. (a) Schematic of LM-WEATHER, each client using *personalized adapter* to endow the PLM for local weather awareness, only low-rank matrices are transmitted to enhance efficiency during communication; (b) Brief structure of PLM on each client, detailed architecture can be found in Appendix; (c) Task Adapter, the multivariate weather series input splits into two paths. The first path isolates the trend, seasonal, and residual elements, which each go through independent generator to produce specific adapters; (d) Architecture of the generator for each decomposed element; (e) Schematic diagram of Channel-Independent Patching [6].

Federated Learning (FL) [7] is a promising on-device intelligence implementation that collaboratively train a uniform model across devices without exchanging raw data. However, the model often underperform due to data heterogeneity among clients. Personalized FL (PFL) provides new insights for on-device intelligence that allows each device obtains customized models for providing personalized insights [8, 9]. Albeit PFL methods showing revolutionized capability in this field, we argue that the current advancements are not necessarily at their best in on-device meteorological variable modeling as three major obstacles remain and hinder further progress:

- (i) **Challenge of heterogeneity.** Weather data’s heterogeneity, unlike that of images or text, arises mainly from the unique characteristics of data collected by weather devices in various regions, such as tropical or arid areas. Furthermore, sensor malfunctions or extreme events can lead to collection disruptions or inconsistent missing data, which significantly increase the differences in data distribution across devices.
- (ii) **Underperformed shallow network structures.** The vast and varied data gathered by weather devices challenge simpler neural network models to generalize effectively. Furthermore, the frequent updates of weather data (hourly or by the minute) require neural models on devices to train and infer more often. This demand is hard to meet with deeper models that, while more performant, are also more resource-intensive.

- (iii) **Resource-constrained weather devices.** From a computation perspective, weather devices cannot afford of training complex neural models from scratch, especially for foundation models [4]. From a communication perspective, transmitting complete model during the aggregation phase in FL/PFL significantly increases communication overhead, which is impractical for real-time weather modeling.

Therefore, a compact foundational model (FM) is crucial for personalized on-device weather modeling. Yet, there’s a gap in FMs for observational data. Models trained on large-scale simulation data struggle in practical applications because of notable differences in data formats and parameter scales [1, 4].

Inspired by the impressive progress of large language models (LLMs) in natural language processing, recent literature in time series analysis research has also demonstrated that pre-trained LMs provide excellent performance over dedicated models for time series analysis with tuning [10] or reprogramming [11]. This comprehensive and thorough sequence knowledge from language models can be effortlessly transferred across domains without large-scale parameter tuning. Thus, an exciting research question naturally arises:

Since PLMs are powerful sequence modelers, can we leverage PLMs as foundation models to achieve personalized on-device meteorological variable modeling?

In this paper, we show that pre-trained language models (PLMs) can as outstanding foundation models that tuned on each device with low cost can achieve personalized on-device weather pattern modeling. We propose LM-WEATHER, a generic approach to taming PLMs to understand heterogeneity on-device weather data. As shown in **Fig.1F**, we conduct a local tuning on an uniform PLM (e.g., GPT2), where lightweight *personalized adapters* are implanted to endow PLMs with weather pattern awareness by decomposing weather sequence to implicit knowledge (e.g., seasonal, trend). During communication between client and server, fewer parameters are shared globally while locally retained adapters are enforced to resist heterogeneity and facilitate privacy-assured fusion of global knowledge.

We highlight our contributions and findings as follows:

- We introduce LM-WEATHER, a generic approach that transforms Pre-trained Language Models as the foundation model to customized on-device meteorological variable modeling via *personalized adapter*. LM-WEATHER yields preferable meteorological variable sequences modeling, while being parameter-, communication-, and data-efficient.
- We collect and compile four real-world versatile datasets for on-device meteorological variable modeling across regions. As opposed to simulated datasets such as ERA5 [12], our datasets are all real-time observations. These datasets based on real-world practice and challenging, provide a pioneer in the field of on-device meteorological variable modeling.
- Experiments show that LM-WEATHER advances the state-of-the-art methods by a large margin across various setting while keeping **3.7%** of parameters communication. LM-WEATHER also demonstrates superior communication efficiency in the context of meteorological variable modeling, beating FL baselines tailored to reduce communication overhead.
- In particular, we find that LM-WEATHER can accurately handle structurally non-deterministic sequences (e.g., differences in time or variable dimensions across devices) thanks to the learned sequences knowledge from pre-trained LMs. We also find that LM-WEATHER can indeed be spatio-temporal sequences sensitive, thereby better modeling the weather pattern specificity of those high distribution similarity.
- We find that LM-WEATHER can work well in data-limited environments across various few-shot settings. We further evaluate zero-shot generalizability of LM-WEATHER in modeling complex weather patterns of unseen data, including different group of datasets and other devices, and observe superb performance.

We highlight that the goal of this study is not to compete but instead to complement current on-device meteorological variables modeling framework. Today’s climate foundation models are typically trained from scratch, utilizing exceptionally large datasets (nearly 100TB [4, 13]) and incurring substantial computational costs [1]. We hope that LM-WEATHER offers a cost-effective alternative for modeling meteorological variables on-device, thereby enabling accurate regional weather trend analysis. In addition, the dataset we compiled can be the important resource to provide exploring chances for this field, facilitating future research.

2 Preliminaries

2.1 On-device Meteorological Variable (Sequence) Modeling

The on-device meteorological variable (sequence) modeling challenge involves predicting future sequences from past observations for forecasting or identifying missing values for imputation on each device. While traditional physics-based methods approach this as a complex problem of solving multilevel atmospheric equations [14], recent deep learning (DL) techniques have shown significant potential in uncovering patterns for better weather prediction [4, 2].

Problem Formulation. On-device meteorological variable modeling can be formulated as an end-to-end sequence-to-sequence learning problem for each device without exchange raw data. Formally, a parameterized local model for i -th device \mathcal{M}_θ^i is tasked with predicting the weather sequence,

$$\mathcal{M}_\theta^i : \mathcal{X}_i \rightarrow \hat{\mathcal{X}}_i \quad (1)$$

where the $\mathcal{X}_i \in \mathbb{R}^{L \times C}$ and $\hat{\mathcal{X}}_i \in \mathbb{R}^{L' \times C'}$ denote the input and output sequences on i -device, L and L' is the input length and output length, C and C' is the number of input and output variable. Note that the $L' \rightarrow L$ when performing imputation. The local learning objective on each device is to find the model parameter θ that minimize the distance between $\hat{\mathcal{X}}_i$ and \mathcal{X}_i given sufficient weather sequence data. The overall optimization objective is based on FedAvg,

$$F(\theta) := \arg \min \sum_{i=1}^N \frac{n_k}{n} F_i(\theta_i | \{D_i\}), \quad (2)$$

where n_i and n is the number of samples held by the k -th device and all clients, respectively, $F(\theta | \{D\})$ denotes the local objective function, $\{D\}$ is the local data.

2.2 Language Models in Time Series

Language models (LMs) trained on large-scale sequence data have shown extraordinary advances and led to a significant paradigm shift in NLP, boosting machines in understanding human languages (BERT/MLM-style) and synthesizing human-like text (GPT/CLM-style [15]). Analogies between time series and human languages have long been noted [16]. Recent advancements in time series analysis have demonstrated the effectiveness of PLMs in modeling time series [17, 11]. Although some of those have shown that PLMs can beat time series-specific models in updating a minor fraction of parameters [18]. As such, it is exciting to expect cutting-edge techniques of language modeling can tackle weather variables sequence-related problems rather than considering train climate foundation models [4, 1] from scratch that are heavy and expensive, and are trained from simulated data.

3 Taming PLMs for On-device Meteorological Variable (Sequence) Modeling

Overview. We proposed a generic framework named LM-WEATHER that encouraging PLMs to yield accurate prediction while keeping high efficiency for each device. The architecture is illustrated in **Fig. 1**. To endow PLMs with weather pattern awareness, we introduce a lightweight *personalized adapter* into PLMs (e.g., GPT2 [15]) such that the emergent ability of sequence modeling that transferred from text into weather is activated. To achieve cross-domain knowledge transfer with minimal effort while maintaining the sequence modeling capabilities of PLMs as intact as possible, We introduce lightweight operations in it enables both clients and servers to achieve outstanding performance while ensuring optimal computational and communication efficiency.

3.1 Local Training

To better tame PLMs that are tasked with language modeling to achieve personalized weather modeling for heterogeneous devices, our framework is accordingly established in a plug-and-play modular fashion. More concretely, we introduce *personalized adapter* consists of (1) *Task Adapter* from latent weather knowledge and (2) *Parameter Adapter* that converts deep representation from PLMs into weather sequence prediction. Lightweight operations are employed during local training to enhance the computational efficiency.

Task Adapter. To provide PLMs with richer effective information to activate their sequence modeling capabilities in the target knowledge domain, similar to text-based prompts in language to LLMs in NLP, we constructed task adapters by decomposing the input weather sequences into multimodal latent statistical information,

$$\mathcal{X}_{\text{Trend}}^k + \mathcal{X}_{\text{Seasonal}}^k + \mathcal{X}_{\text{Residual}}^k = \text{Decomp}(\mathcal{X}^k), \quad (3)$$

where the $\mathcal{X}^k \in \mathbb{R}^{L \times 1}$ denote the k -th variable in weather sequence $\mathcal{X} \in \mathbb{R}^{L \times C}$, the trend component $\mathcal{X}_{\text{Trend}}$ and the seasonal component $\mathcal{X}_{\text{Seasonal}}$ captures the underlying long-term weather pattern and encapsulates the repeating short-term weather cycles, respectively. Furthermore, the residual component $\mathcal{X}_{\text{Residual}}$ represents the remainder of the sequence after the trend and seasonality have been extracted. Note that $\mathcal{X}_{\text{Trend}}$, $\mathcal{X}_{\text{Seasonal}}$, and $\mathcal{X}_{\text{Residual}}$ have the same shape as \mathcal{X} . This decomposition explicitly enables the identification of unusual observation and shifts in seasonal patterns or trends. The $\mathcal{X}_{\text{Trend}}$, $\mathcal{X}_{\text{Seasonal}}$, $\mathcal{X}_{\text{Residual}}$ are used to generate *Task Adapter* via an unified generator as **the right of Fig. 1C & Fig. 1E** that consisting of Token Embedding, Position Embedding, and Temporal Embedding. Specially, we use one-dimensional convolution operation to map each each specific sample \mathcal{X}^k while keeping raw shape to generate Token Adapter \mathbf{P}_{TO} . Additionally, we use a trainable lookup table to map each point’s explicit position in the entire sequence, to generate Position Adapter \mathbf{P}_{PO} . Furthermore, we separately encode different time attributes such as minutes, hours, days, weeks, and months, via trainable parameters to dynamically model complex temporal shifts, to generate Temporal Adapter \mathbf{P}_{TE} . Finally, for each decomposition components, corresponding generated adapters can be obtained by aggregating Token Adapter $\mathbf{P}_{\text{TO}} \in \mathbb{R}^{L \times C}$, Position Adapter $\mathbf{P}_{\text{PO}} \in \mathbb{R}^{L \times C}$, and Temporal Adapter $\mathbf{P}_{\text{TE}} \in \mathbb{R}^{L \times C}$ as $\mathbf{P}_d = \mathbf{P}_{\text{TO}}^d + \mathbf{P}_{\text{PO}}^d + \mathbf{P}_{\text{TE}}^d$, where $d \in \{\text{Trend, Seasonal, Residual}\}$, this means that we can obtain $\mathbf{P}_{\text{Trend}}$, $\mathbf{P}_{\text{Seasonal}}$, $\mathbf{P}_{\text{Residual}}$. Details about the generator can be found at **Appendix B.5**.

Lightweight Operations. To enhance the PLMs’ ability to represent complex inputs while reducing the computational burden to adapt to low-resource devices, we introduce lightweight operations, which includes channel-independent patching (CIP, **Fig. 1E**) [6] for input and efficient tuning of parameters for PLMs. Among them, CIP splits the multivariate sequence into separate univariate sequences, each processed by a single model with length L_p . This approach outperforms the original method of mixing channels by treating the variables as independent. It enables the model to capture channel interactions indirectly through shared weights, leading to improved performance without directly modeling the complexity of multiple data channels. The total number of inputs patches is $P = \frac{(T-L_p)}{S} + 2$, where S denotes the horizontal sliding stride. Given these patches $\mathcal{X}_P^i \in \mathbb{R}^{P \times L_p}$, we use rearrange operation and a trainable FFN embed them as $\hat{\mathcal{X}}_P^i \in \mathbb{R}^{P \times d_m}$, where d_m is dimensions created by the FFN. We also introduce a low-rank adaptation (LoRA) [19] inside PLMs aiming at language modeling for lightweight fine-tuning of attention layers to achieve cross-modal/-domain knowledge transfer from text sequences to weather sequences with minimal effort.

Parameter Adapter. To transform the representation of PLMs into actual weather sequence predictions, we construct a *Parameter Adapter* based on the FFN attached behind the PLM,

$$\hat{\mathcal{X}} = \text{FFN}(\mathcal{M}_\theta(\text{Concat}[\hat{\mathbf{P}}_{\text{Trend}}, \hat{\mathbf{P}}_{\text{Seasonal}}, \hat{\mathbf{P}}_{\text{Residual}}, \hat{\mathcal{X}}])), \quad (4)$$

where the $\hat{\mathbf{P}}_{\text{Trend}}$, $\hat{\mathbf{P}}_{\text{Seasonal}}$, $\hat{\mathbf{P}}_{\text{Residual}}$, and $\hat{\mathcal{X}}$ are obtained from CIP based on $\mathbf{P}_{\text{Trend}}$, $\mathbf{P}_{\text{Seasonal}}$, $\mathbf{P}_{\text{Residual}}$, and \mathcal{X} . The underlying motivations are: 1) enabling the PLM receive richer cross-modal representations by aggregating task-specific knowledge, 2) forcing the PLM to generate accurate outputs while maintaining sufficient its prior knowledge by feeding weather information to cross-domain knowledge transferring.

3.2 Communication

To avoid data silos, facilitate global knowledge fusion, reduce the negative impact of significant heterogeneity among weather devices on overall performance while maintaining outstanding communication efficiency, we update personalized adapters locally and share low-rank parameters globally; specifically, the PLM \mathcal{M}_θ can be formulated as below according to LoRA,

$$\mathcal{M}_\theta \rightarrow \mathcal{M}_{\theta,f}(\text{Locally}) + \mathcal{M}_{\theta,t}(\text{Communication}) \quad (5)$$

where $\mathcal{M}_{\theta,f}$ is the frozen parameter, and the $\mathcal{M}_{\theta,t}$ denotes the trainable parameter from the low-rank matrices of *query* and *value* in attention modules. During communication between client and server, only $\mathcal{M}_{\theta,t}$ will be transmitted.

4 Theorems

Theorem 4.1 (Decomposition Rationality from Time Series). *Given a weather series $\mathcal{X} = \mathcal{X}_{Trend,t} + \mathcal{X}_{Seasonal,t} + \mathcal{X}_{Residual,t}$, $t \in [t_1, t_n]$. Let $\mathbf{E} = \{e_1, e_2, \dots, e_n\}$ denotes a set of orthogonal bases. Let $\mathbf{E}_{Seasonal} \subseteq \mathbf{E}$ denote the subset of \mathbf{E} on which $\mathcal{X}_{Seasonal,t}$ has non-zero eigenvalues and $\mathbf{E}_{Trend} \subseteq \mathbf{E}$ denote the subset of \mathbf{E} on which $\mathcal{X}_{Trend,t}$ has non-zero eigenvalues. If $\mathcal{X}_{Trend,t}$ and $\mathcal{X}_{Seasonal,t}$ are not orthogonal, i.e., $\sum_{i=1}^n \mathcal{X}_{Trend,t}^i \mathcal{X}_{Seasonal,t}^i \neq 0$, then $\mathbf{E}_{Trend} \cap \mathbf{E}_{Seasonal} \neq \emptyset$, i.e., \mathbf{E} can not disentangle the two signals onto two disjoint set of bases.*

Theorem 4.2 (Exchange Low-Rank Matrices Ensures Privacy). *Given a on-device weather modeling framework based on federated learning that gloabl optimization object is $\mathbf{F}(\theta) = \sum_{i=1}^n p_i f(\{D_i\}; \theta)$, where $f(x; \theta)$ is the loss function of i -th client, $\{D_i\}$ is dataset of i -th client, and p_i and θ denote the data distribution weight of client i and the model parameters, respectively. Given that the parameters θ of the PLM \mathcal{M}_θ broadcasted by the server consist of two parts: a frozen part $\mathcal{M}_{\theta,f}$ and a trainable part $\mathcal{M}_{\theta,t}$, interacting only the low-rank matrix parameters $\mathcal{M}_{\theta,l} \subset \mathcal{M}_{\theta,t}$ is a subset of trainable part $\mathcal{M}_{\theta,t}$ during each round ensures privacy.*

5 Experiments

In this section, we first present the real-world datasets that we have collected and compiled for on-device meteorological variable modeling, and second, we evaluate LM-WEATHER on these datasets, which involves normal scenario, a data-limited few-shot scenario, and a zero-shot scenario with no training data (OOD). Please refer to **Appendix** for more detailed information about proposed datasets and additional results of all evaluations (e.g., full results, additional findings & experiments).

5.1 Datasets

Despite the proliferation of reanalysis data aimed at building frameworks for global climate analysis, these datasets often struggle to model regional weather trend due to: (1) they depend on numerous simulations of atmospheric equations, introducing biases inconsistent with real observations, and (2) they face challenges in refining their scale to suit specific regional applications. Hence, we collected real observational data from various weather stations across different regions. We then organized this data into two series, each comprising two distinct datasets, to underscore the heterogeneity inherent in real-world settings. For detailed information on these datasets, please see the **Appendix B.1**.

On-device Weather Series 1# (ODW1). The dataset gathered from 15 ground weather stations across China, Japan, and South Korea, encompasses over 20 variables. It has been divided into two subsets: **ODW1T** has a heterogeneous time span, meaning the data collection start and end times vary by location. and **ODW1V** extends **ODW1T** by adding variability in the observed variables; while one variable remains constant at each station, the others vary.

On-device Weather Series 2# (ODW2). This dataset consists of data from 36 weather observation stations in the United States, Canada, and Israel, covering 5 different variables with a temporal resolution of 1 hour. Following the dataset setting of **ODW1**, the dataset was also subdivided into two different dataset, including **ODW2T** and **ODW2V**.

5.2 Setup

Baseline. Since our framework is based on a language model, we compare with DL-based SOTA time series models, including Transformer-based methods: Transformer [20], Informer [3], Reformer [21], Pyraformer [22], iTransformer [23], and PatchTST [6], and recent competitive models: GPT4TS [17], DLinear [24] and LightTS [25]. Note that our setting is FL-based, so we place them in FL and rename them FL-(baseline) like FL-Transformer, etc., and all aggregation methods used in above models is FedAvg [7]. In addition, we report a variants of LM-WEATHER, LM-WEATHER-AVE that based on FedAvg without personalization. Detailed information are in **Appendix B.2**.

Basic Setup. We focus on on-device meteorological variable forecasting and imputation tasks. For forecasting, we create scenarios for predicting a single variable (multivariate-univariate) and for predicting all variables (multivariate-multivariate). The main text only includes multivariate-to-multivariate forecasting results due to page constraints. For multivariate-to-univariate forecasts, refer

to the Appendix E. In imputation, we use sequence lengths of $\{96, 192, 336, 720\}$ and apply three different masking probabilities $\{25\%, 35\%, 50\%\}$ to represent missing data. The main manuscript shows imputation results for a 50% masking ratio. For more details on the setup, please refer to **Appendix B.3**. All our experiments are repeat five times and we report the averaged results.

5.3 Main Results

In this section, we evaluate LM-WEATHER and baseline methods on four on-device meteorological variable modeling datasets in general experiments to validate its effectiveness.

Setups & Results of Forecasting Tasks. Input length L_b is fixed to 192, and we use four different prediction horizons $L_f \in \{96, 192, 336, 720\}$. Evaluation metrics include mean absolute error (MAE) and root square mean error (RMSE). The brief results is shown in **Tab. 1**, where our LM-WEATHER outperforms all baselines in most cases and significantly so to the majority of them. Particularly noteworthy is the comparison with GPT4TS that involves fine-tuning PLMs, where LM-WEATHER has an average **9.8%** improvement over FL-GPT4TS (MAE reported), and even the variant LM-WEATHER-AVE has an average **4%** improvement over FL-GPT4TS. In addition, LM-WEATHER shows significant average performance gains of **11.2%** and **19%** w.r.t. MAE relative to other SOTA such as FL-DLinear and FL-PatchTST.

Table 1: Results under on-device meteorological variable forecasting task (multivariate-to-multivariate). A lower value indicates better performance. **Bold**: the best, Underline: the second best. **Complete results can be found at Appendix E due to page limitation.**

Method	LM-WEATHER-AVE	LM-WEATHER	FL-GPT4TS	FL-Reformer	FL-Pyraformer	FL-DLinear	FL-PatchTST	FL-iTransformer	FL-LightTS	FL-Transformer	FL-Informer
Dataset	Length	MAE	RMSE	MAE	RMSE	MAE	RMSE	MAE	RMSE	MAE	RMSE
ODW1T	96	<u>44.1</u>	<u>74.8</u>	42.3	71.1	46.3	78.5	70.7	92.9	67.2	86.1
	192	<u>46.3</u>	<u>72.5</u>	44.4	73.6	48.6	81.3	75.1	98.3	70.0	90.9
	336	<u>47.9</u>	<u>79.3</u>	45.8	75.2	50.3	83.2	79.8	100.5	74.1	92.8
	720	<u>51.8</u>	<u>83.0</u>	49.2	78.5	54.4	87.2	87.1	102.9	80.5	95.2
	Avg.	<u>47.5</u>	<u>78.7</u>	45.4	74.6	49.9	82.5	78.2	98.7	73.0	91.3
ODW1V	96	<u>42.7</u>	<u>69.5</u>	42.3	69.6	44.0	71.4	42.9	<u>67.8</u>	57.7	<u>67.2</u>
	192	<u>45.5</u>	<u>72.6</u>	44.4	71.7	47.0	75.8	48.4	75.4	59.2	<u>69.4</u>
	336	<u>47.2</u>	<u>74.3</u>	46.0	72.4	48.8	77.7	51.0	77.0	63.4	<u>73.3</u>
	720	<u>51.2</u>	<u>78.2</u>	49.7	74.0	53.2	81.7	54.5	82.3	67.3	<u>76.1</u>
	Avg.	<u>46.6</u>	<u>73.6</u>	45.6	71.9	48.3	76.7	49.2	75.6	61.9	<u>71.5</u>
ODW2T	96	<u>64.3</u>	<u>88.2</u>	62.8	85.5	66.8	91.7	100.3	<u>126.3</u>	95.0	<u>120.3</u>
	192	<u>67.7</u>	<u>91.5</u>	66.2	89.1	71.1	96.1	102.1	<u>130.3</u>	99.9	<u>125.8</u>
	336	<u>69.5</u>	<u>93.7</u>	67.9	91.1	72.9	98.4	104.2	<u>130.0</u>	102.0	<u>128.5</u>
	720	<u>72.6</u>	<u>97.3</u>	70.7	94.6	76.2	101.2	107.3	<u>134.2</u>	104.2	<u>131.4</u>
	Avg.	<u>68.5</u>	<u>92.7</u>	66.9	90.1	71.8	96.9	103.5	<u>130.2</u>	100.3	<u>126.5</u>
ODW2V	96	<u>76.8</u>	<u>99.7</u>	75.1	88.4	78.5	102.7	89.6	<u>112.7</u>	89.1	<u>112.5</u>
	192	<u>77.9</u>	<u>100.8</u>	76.3	91.4	79.7	103.8	90.5	<u>114.2</u>	96.4	<u>120.1</u>
	336	<u>78.5</u>	<u>101.5</u>	76.9	93.0	80.3	104.5	94.2	<u>119.3</u>	98.4	<u>122.2</u>
	720	<u>79.9</u>	<u>103.6</u>	77.9	96.5	82.0	106.7	97.4	<u>120.4</u>	100.5	<u>125.0</u>
	Avg.	<u>78.3</u>	<u>101.4</u>	76.0	92.3	80.1	104.4	92.9	<u>116.6</u>	96.1	<u>120.0</u>
1 st Count	0		29		0		0		6		0

Setups & Results of Imputation Tasks. Our brief results are in **Tab. 2**, where LM-WEATHER consistently surpasses all baselines, outperforming FL-GPT4TS by **5.7%**. LM-WEATHER remains competitive even when compared with the SOTA, FL-PatchTST, FL-LightTS, and FL-DLinear.

Table 2: Results under on-device meteorological variable imputation task, where random masking ratio is 50%. A lower value indicates better performance. **Bold**: the best, Underline: the second best. **Complete results can be found at Appendix E due to page limitation.**

Method	LM-WEATHER-AVE	LM-WEATHER	FL-GPT4TS	FL-Reformer	FL-Pyraformer	FL-DLinear	FL-PatchTST	FL-iTransformer	FL-LightTS	FL-Transformer	FL-Informer
Dataset	Length	MAE	RMSE	MAE	RMSE	MAE	RMSE	MAE	RMSE	MAE	RMSE
ODW1T	96	<u>22.4</u>	<u>43.5</u>	21.7	41.8	23.3	45.2	63.7	88.4	63.2	85.9
	192	<u>22.4</u>	<u>43.7</u>	22.6	42.0	24.6	45.9	67.2	91.2	65.5	88.5
	336	<u>24.1</u>	<u>44.1</u>	23.2	42.4	25.3	46.3	70.4	93.4	68.5	90.6
	720	<u>26.0</u>	<u>44.1</u>	24.9	43.3	27.3	47.4	77.9	96.8	75.8	93.9
	Avg.	<u>24.0</u>	<u>44.1</u>	23.1	42.4	25.1	46.2	69.8	92.5	68.0	89.7
ODW1V	96	<u>42.1</u>	<u>62.0</u>	41.1	60.4	42.9	63.8	43.8	64.9	42.3	<u>53.0</u>
	192	<u>43.9</u>	<u>64.5</u>	42.8	62.8	45.6	66.9	45.8	67.6	44.7	<u>56.2</u>
	336	<u>45.7</u>	<u>66.6</u>	44.6	64.9	47.5	69.2	47.6	69.8	54.6	<u>65.7</u>
	720	<u>47.5</u>	<u>68.7</u>	46.3	66.9	49.4	71.4	49.6	72.0	59.2	<u>73.5</u>
	Avg.	<u>44.8</u>	<u>65.6</u>	43.7	63.8	46.4	67.8	46.7	68.6	50.2	<u>62.1</u>
ODW2T	96	<u>38.0</u>	<u>56.5</u>	36.9	54.9	39.1	58.3	50.3	70.3	95.4	<u>120.8</u>
	192	<u>38.3</u>	<u>56.6</u>	37.2	54.9	39.8	58.9	52.1	74.2	96.2	<u>122.3</u>
	336	<u>43.5</u>	<u>65.5</u>	42.2	63.5	44.8	68.1	56.6	78.9	97.8	<u>125.5</u>
	720	<u>47.9</u>	<u>68.8</u>	46.5	66.7	49.8	71.5	64.3	87.7	99.1	<u>129.9</u>
	Avg.	<u>41.9</u>	<u>61.9</u>	38.8	61.7	43.4	64.2	55.8	77.8	97.1	<u>124.6</u>
ODW2V	96	<u>28.0</u>	<u>45.3</u>	27.5	44.0	28.4	45.8	50.3	70.3	53.2	<u>72.4</u>
	192	<u>28.6</u>	<u>45.3</u>	28.0	44.0	29.2	46.1	51.0	71.1	46.1	<u>65.2</u>
	336	<u>33.7</u>	<u>49.8</u>	32.7	48.4	34.9	51.8	54.2	76.6	74.2	<u>97.3</u>
	720	<u>37.1</u>	<u>53.1</u>	36.0	51.5	39.3	56.3	59.4	81.7	82.4	<u>100.9</u>
	Avg.	<u>31.9</u>	<u>48.4</u>	31.1	47.0	33.0	50.0	53.7	74.9	64.0	<u>84.0</u>
1 st Count	0		30		0		0		0		0

5.4 Few-Shot Learning Experiments

PLMs have demonstrated remarkable few-shot learning capabilities [26]. In this subsection, we assess whether LM-WEATHER retains this ability in both forecasting and imputation tasks, based on FL for resource-constrained on-device weather modeling environments.

Table 3: Few-Shot learning results on forecasting task (5% training data). A lower value indicates better performance. **Bold**: the best, Underline: the second best. **More and complete results can be found at Appendix E.2** - denotes insufficient data.

Method		LM-WEATHER-AVE		LM-WEATHER		FL-GPT4TS		FL-Reformer		FL-Pyraformer		FL-DLinear		FL-PatchTST		FL-tTransformer		FL-Lights		FL-Transformer		FL-Informer	
Metrics	Length	MAE	RMSE	MAE	RMSE	MAE	RMSE	MAE	RMSE	MAE	RMSE	MAE	RMSE	MAE	RMSE	MAE	RMSE	MAE	RMSE	MAE	RMSE	MAE	RMSE
ODW1T	96	88.1	95.1	<u>87.3</u>	93.9	91.6	100.9	166.9	296.0	173.6	299.2	92.4	187.5	88.1	182.7	103.3	204.8	185.8	328.3	93.7	193.5	91.1	190.0
	192	90.2	98.4	89.6	96.5	95.8	104.6	166.9	297.3	176.0	303.0	94.4	192.4	90.7	191.6	106.7	210.7	188.1	336.0	96.8	200.1	93.5	195.9
	336	<u>94.2</u>	<u>101.7</u>	92.2	99.7	100.0	108.2	168.9	297.5	177.6	303.0	95.9	193.2	96.5	197.4	108.7	211.8	188.4	334.6	100.2	203.3	99.3	201.0
	720	-	-	-	-	-	-	-	-	-	-	-	-	-	-	-	-	-	-	-	-	-	-
Avg.		<u>90.8</u>	98.4	89.7	96.7	95.8	104.6	167.7	296.9	175.7	301.7	94.2	191.0	90.7	<u>190.6</u>	106.3	209.1	187.5	333.0	96.9	199.0	94.6	195.6
ODW1V	96	79.6	<u>104.3</u>	75.7	98.1	82.0	108.5	101.5	130.2	81.6	107.5	98.8	127.4	327.6	392.4	135.0	168.3	111.0	141.6	116.6	155.8	111.5	144.9
	192	<u>87.8</u>	<u>115.5</u>	82.5	108.4	90.8	120.3	107.0	136.7	90.2	118.9	110.4	141.6	334.4	403.4	145.4	180.2	117.5	149.2	123.4	164.1	116.0	152.4
	336	<u>103.9</u>	<u>133.4</u>	98.7	125.4	107.0	138.7	113.2	142.4	106.1	137.5	120.0	153.2	341.6	413.7	122.1	153.5	126.3	159.7	133.6	161.3	123.2	167.4
	720	-	-	-	-	-	-	-	-	-	-	-	-	-	-	-	-	-	-	-	-	-	-
Avg.		<u>90.4</u>	<u>117.7</u>	85.6	110.6	93.3	122.5	107.2	136.4	92.6	121.3	109.7	140.7	334.5	403.2	134.2	167.3	118.3	150.2	124.5	160.4	116.9	154.9
ODW2T	96	111.0	159.4	99.0	135.5	127.9	178.2	158.3	241.2	173.3	247.1	107.1	152.8	<u>101.2</u>	<u>147.9</u>	115.9	166.3	183.6	273.3	142.3	199.6	158.8	201.3
	192/336/720	-	-	-	-	-	-	-	-	-	-	-	-	-	-	-	-	-	-	-	-	-	-
	Avg.		111.0	159.4	99.0	135.5	127.9	178.2	158.3	241.2	173.3	247.1	107.1	152.8	<u>101.2</u>	<u>147.9</u>	115.9	166.3	183.6	273.3	142.3	199.6	158.8
ODW2V	96	105.3	<u>135.7</u>	96.8	122.1	110.2	155.4	151.5	190.7	150.5	189.3	112.2	141.2	115.5	145.8	110.2	143.4	162.1	212.5	106.4	136.8	149.6	188.2
	192/336/720	-	-	-	-	-	-	-	-	-	-	-	-	-	-	-	-	-	-	-	-	-	-
	Avg.		<u>105.3</u>	<u>135.7</u>	96.8	122.1	110.2	155.4	151.5	190.7	150.5	189.3	112.2	141.2	115.5	145.8	110.2	143.4	162.1	212.5	106.4	136.8	149.6
1 st Count		1		16		0		0		0		0		2		0		0		0		0	

Table 4: Few-Shot learning results on imputation task (5% training data), where random masking ratio is 50%. A lower value indicates better performance. **Bold**: the best, Underline: the second best. **Appendix E.2 shows our full results.** - denotes insufficient data.

Method		LM-WEATHER-AVE		LM-WEATHER		FL-GPT4TS		FL-Reformer		FL-Pyraformer		FL-DLinear		FL-PatchTST		FL-tTransformer		FL-LightTS		FL-Transformer		FL-Informer	
Ratio	Length	MAE	RMSE	MAE	RMSE	MAE	RMSE	MAE	RMSE	MAE	RMSE	MAE	RMSE	MAE	RMSE	MAE	RMSE	MAE	RMSE	MAE	RMSE	MAE	RMSE
ODW1T	96	61.2	121.2	59.9	120.8	62.4	138.6	147.4	261.3	149.5	256.4	110.0	209.1	64.2	147.0	119.0	228.5	173.0	310.8	140.8	260.0	143.9	264.7
	192	69.1	<u>130.2</u>	64.7	127.7	<u>62.3</u>	145.2	151.3	267.8	152.0	258.1	110.1	203.4	74.1	155.1	120.9	223.0	172.2	301.4	149.1	262.4	150.3	264.2
	336/720	-	-	-	-	-	-	-	-	-	-	-	-	-	-	-	-	-	-	-	-	-	-
	Avg.		65.2	<u>125.7</u>	62.3	124.4	<u>64.9</u>	141.9	149.4	264.6	150.8	257.3	110.0	206.2	69.2	151.0	120.0	225.7	172.6	306.1	145.0	261.2	147.1
ODW1V	96	62.2	134.1	62.8	135.5	67.3	131.2	103.9	189.8	61.5	<u>132.6</u>	112.2	208.4	161.1	281.5	117.6	219.5	119.6	223.5	98.0	198.5	94.2	188.1
	192	<u>71.4</u>	<u>140.5</u>	72.2	142.1	74.6	152.7	103.3	182.4	70.6	138.8	113.3	200.6	160.5	272.4	124.5	218.9	122.7	217.8	101.8	191.3	96.7	181.5
	336/720	-	-	-	-	-	-	-	-	-	-	-	-	-	-	-	-	-	-	-	-	-	-
	Avg.		<u>66.8</u>	<u>137.3</u>	67.5	138.8	71.0	142.0	103.6	186.1	66.1	135.7	112.7	204.5	160.8	276.9	121.0	219.2	121.2	220.7	101.8	194.9	95.5
ODW2T	96	102.5	<u>156.3</u>	99.4	151.6	112.0	157.2	116.2	161.3	124.9	165.6	123.7	178.3	173.0	256.7	127.3	190.6	133.8	200.3	124.3	187.5	105.7	161.1
	192/336/720	-	-	-	-	-	-	-	-	-	-	-	-	-	-	-	-	-	-	-	-	-	-
	Avg.		<u>102.5</u>	<u>156.3</u>	99.4	151.6	112.0	157.2	116.2	161.3	124.9	165.6	123.7	178.3	173	256.7	127.3	190.6	133.8	200	124.3	188	105.7
ODW2V	96	42.4	<u>62.9</u>	35.7	112.1	56.4	77.3	106.8	135.5	70.8	95.5	113.3	148.0	153.8	199.5	101.8	136.4	106.1	142.2	100.1	134.6	89.8	119.0
	192/336/720	-	-	-	-	-	-	-	-	-	-	-	-	-	-	-	-	-	-	-	-	-	-
	Avg.		<u>42.4</u>	<u>62.9</u>	35.7	112.1	56.4	77.3	106.8	135.5	70.8	95.5	113.3	148.0	153.8	199.5	101.8	136.4	106.1	142.2	100.1	134.6	89.8
1 st Count		0		12		1		0		6		0		0		0		0		0		0	

Setups and Results of Forecasting & Imputation. For both forecasting and imputation tasks, we evaluate the few-shot learning capability in scenarios using limited data, specifically, we use training ratios of 5% and 15% (Our full few-shot learning results (training ratio of 5% and 15%) can be found at **Appendix E.2**). The brief 5% few-shot learning results on forecasting and imputation tasks are depicted in **Tab. 3** and **Tab. 4**, respectively. LM-WEATHER remarkably excels over all baseline methods, and we attribute this to the successful cross-domain knowledge activation in our local dual fine-tuning for the PLM. In addition, our LM-WEATHER’s communication mechanism also reduces the impact of data heterogeneity on performance, which is reflected in the fact that LM-WEATHER has an average **14.7%** and **20%** improvement relative to LM-WEATHER-AVE, in the forecasting and imputation, respectively. In relation to recent SOTA methods such as FL-PatchTST, FL-LightTS, and FL-DLinear, our LM-WEATHER enhancements surpass **78%**, **14.3%**, and **72.8%** for forecasting, and **102.1%**, **122.1%**, and **96.35%** for imputation. This means that heterogeneity poses challenge to baseline and they struggle to understand weather patterns with limited data. Moreover, it implies that LM-WEATHER can effectively achieve cross-domain knowledge transfer to PLMs. This benefits from the personalized adapter we integrated into the PLM, coupled with lightweight operations.

5.5 Zero-Shot Learning (Out of Distribution Modeling) Experiments

Beyond few-shot learning, PLMs hold potential as effective zero-shot reasoners. We evaluate the zero-shot learning capabilities of LM-WEATHER within the framework of cross-domain adaption. Specifically, we examine how well a method performs on a dataset when it is optimized on another dataset, where the model has not encountered any data samples from the original dataset. We use forecasting/imputation protocol and evaluate on various cross-domain scenarios. Note that we choose LM-WEATHER-AVE rather than LM-WEATHER for comparison due to it can obtain a unified model for zero-shot experiments whereas LM-WEATHER is obtain multiple personalized models. The results are in **Tab. 5**. LM-WEATHER-AVE consistently outperforms the most competitive baselines by a large margin, over **14.2%** and **14.2%** w.r.t the second-best in MAE reduction, in forecasting and imputation, respectively. We attribute this to our personalized adapter that we implant in PLMs being better at activating the PLM’s knowledge transfer and domain-adaption capabilities in a resource-efficient manner when modeling weather variables.

Table 5: Results on Zero-Shot Learning (ave. MAE report). **Bold**: the best, Underline: the second best, ⇔: domain transferring.

Setting	Task	LM-WEATHER-AVE	FL-GPT4TS	FL-DLinear	FL-PatchTST
OWD1T ⇔ ODW1V	fore.	<u>54.2</u>	59.4	50.2	67.4
	imp.	<u>48.9</u>	48.4	54.9	69.5
OWD1T ⇔ ODW2V	fore.	<u>92.1</u>	89.9	99.4	96.7
	imp.	33.2	34.2	80.4	56.4
OWD1T ⇔ OWD2T	fore.	80.4	<u>87.4</u>	94.8	86.5
	imp.	48.4	<u>53.5</u>	67.2	71.1
OWD2T ⇔ ODW2V	fore.	84.9	<u>88.2</u>	106.5	92.1
	imp.	33.3	<u>36.4</u>	99.1	55.5
OWD2T ⇔ ODW1V	fore.	57.7	<u>58.3</u>	69.1	74.2
	imp.	<u>49.6</u>	47.5	75.3	71.1
OWD2T ⇔ OWD1T	fore.	59.5	63.1	78.3	<u>61.2</u>
	imp.	25.5	<u>27.1</u>	57.1	38.6
ODW1V ⇔ ODW2V	fore.	90.1	<u>96.7</u>	114.2	104.7
	imp.	<u>36.9</u>	27.2	101.2	59.2
ODW1V ⇔ OWD2T	fore.	79.3	<u>84.5</u>	96.9	89.7
	imp.	46.1	<u>47.5</u>	71.2	77.4
ODW1V ⇔ OWD1T	fore.	51.2	<u>53.8</u>	67.7	56.4
	imp.	25.8	<u>27.2</u>	54.0	32.7
ODW2V ⇔ ODW1V	fore.	56.0	<u>58.5</u>	70.4	72.7
	imp.	51.8	<u>54.2</u>	74.2	69.9
ODW2V ⇔ OWD1T	fore.	59.5	63.1	72.9	<u>60.4</u>
	imp.	29.6	<u>30.9</u>	59.8	39.9
ODW2V ⇔ OWD2T	fore.	72.1	<u>76.9</u>	87.4	80.5
	imp.	<u>44.3</u>	41.2	66.7	65.7
1 st Count		18	5	1	0

Table 6: Ablation results on forecasting (multivariate to multivariate) and imputation (50% masking ratio, **OWD1T** dataset). A lower value indicates better performance. **Bold**: the best, Underline: the second best, ↓ and ↑ denote performance degradation and performance improvement, respectively.

Method	Task		Ablation Perspective		Ave. Variations		Params.#	
	Forecasting	Imputation	Model Component	Personalized Method	Forecasting	Imputation	Train.#	Comm.#
LM-WEATHER	45.4/74.6	23.1/40.0	Original	Original	-	-	10.38 M	0.38 M
LM-WEATHER-A	50.8/87.6	26.0/47.7	wo Decomposition	Original	↓ 11.8%	↓ 12.6%	10.38 M	0.38 M
LM-WEATHER-B	50.9/85.6	25.4/47.1	wo Trend Component	Original	↓ 12.1%	↓ 10.0%	10.37 M	0.38 M
LM-WEATHER-C	50.1/83.6	25.0/46.1	wo Seasonal Component	Original	↓ 10.3%	↓ 8.2%	10.37 M	0.38 M
LM-WEATHER-D	49.3/81.7	24.4/45.6	wo Residual Component	Original	↓ 8.6%	↓ 5.6%	10.37 M	0.38 M
LM-WEATHER-E	53.8/95.6	25.5/47.0	wo Prompt Generator	Original	↓ 18.5%	↓ 10.4%	10.36 M	0.38 M
LM-WEATHER-F	49.4/82.3	28.1/52.0	Original	w LoRA, Local: Low-Rank Matrix, Global: the rest of trainable param.	↓ 8.8%	↓ 21.6%	10.38 M	10.00 M
LM-WEATHER-G	43.2/71.4	22.4/39.1	Original	wo LoRA, Local: Attention Param, Global: Attention Param	↑ 5.1%	↑ 3.1%	52.01 M	41.99 M
LM-WEATHER-H	42.7/71.2	22.2/39.3	Original	wo LoRA, Local: Attention Param, Global: the rest of trainable param.	↑ 6.3%	↑ 4.1%	52.01 M	10.00 M

5.6 Framework Analysis Experiments

We demonstrate the effectiveness of LM-WEATHER through experiments focused on ablation studies and parameter comparison. For detailed results and further analysis (*e.g.*, hyper-parameter, additional findings and discussion), please refer to the **Appendix D** and **Appendix E**.

Ablation Study. Follow the setting of main experiments, we report our brief ablation results in **Tab. 6**, please refer to **Appendix E.3** for full results. The results indicate a notable drop in performance when we omit the weather decomposition components (LM-WEATHER-A/B/C/D). Additionally, keeping the decomposition term but removing the associated generator leads to a 14.5% average performance decline. This suggests that our personalized adapter effectively leverages the PLM’s modeling of weather data. Conversely, when we alter the personalized approach by changing the shared low-rank matrix to other trainable parameters (LM-WEATHER-F), we observe a significant performance drop and increased communication costs. Furthermore, moving from LoRA to fully fine-tuning the attention parameters results in a slight performance gain but incurs over four times the parameter count and a massive increase in communication overhead, which is inefficient for us. These outcomes highlight the benefits of the personalized adapter.

Parameter Comparison. The results are shown in **Tab. 7**. LM-WEATHER ensures top while only communicate about **3.7%** of the trainable parameters, compared to the baseline that communicates the

Table 7: Experiment results on parameter comparison (ave. MAE/RMSE report), **Bold**: the best.

Method	Task		Params.#		
	Forecasting	Imputation	Train.	Comm.	Ratio
LM-WEATHER	45.4/74.6	23.1/42.2	10.38 M	0.38 M	3.70%
FL-GPT4TS	49.9/82.5	25.1/46.2	12.42 M	12.42 M	100%
FL-Reformer	78.2/98.7	69.8/92.5	19.74 M	19.74 M	100%
FL-Pyraformer	73.0/91.3	68.0/89.7	153.32 M	153.32 M	100%
FL-DLinear	63.3/82.8	28.5/49.9	1.06 M	1.06 M	100%
FL-PatchTST	48.6/81.0	45.4/73.5	74.74 M	74.74 M	100%
FL-Itrransformer	53.7/63.7	27.6/48.2	26.74 M	26.74 M	100%
FL-LightTS	62.7/93.4	26.1/45.7	1.68 M	1.68 M	100%
FL-Transformer	52.8/84.7	57.6/82.3	45.55 M	45.55 M	100%
FL-Informer	53.4/85.2	61.4/85.9	52.31 M	52.31 M	100%

full model parameters. When compared with competitive methods, FL-DLinear and FL-LightTS, LM-WEATHER’s communication overhead is just **35.9%** and **22.6%** of theirs, respectively, highlighting LM-WEATHER’s superior communication efficiency.

6 Conclusion and Future Works

This paper demonstrate that pre-trained language models (PLMs) are strong foundation models for personalized on-device meteorological variable modeling. We propose LM-WEATHER, a generic framework to taming PLMs to acquire highly customized models for heterogeneous meteorological data on devices while keeping high efficiency. Concretely, we introduce a lightweight personalize adapter into PLMs and endow it with weather pattern awareness. Experiments on real-world datasets demonstrate that LM-WEATHER outperforms the SOTA results by a large margin across various tasks. In addition, extensive analyses indicate that LM-WEATHER can (1) effectively achieve cross-domain knowledge transfers, (2) render device with highly customized model while keeping high efficiency, and (3) generalize under few-shot and zero-shot scenario. In future work, we plan to extend LM-WEATHER to multimodal weather data (text/image/time-series) and to finer scales.

References

- [1] Tung Nguyen, Johannes Brandstetter, Ashish Kapoor, Jayesh K Gupta, and Aditya Grover. Climax: A foundation model for weather and climate. *arXiv preprint arXiv:2301.10343*, 2023.
- [2] Ryan Keisler. Forecasting global weather with graph neural networks. *arXiv preprint arXiv:2202.07575*, 2022.
- [3] Haoyi Zhou, Shanghang Zhang, Jieqi Peng, Shuai Zhang, Jianxin Li, Hui Xiong, and Wancai Zhang. Informer: Beyond efficient transformer for long sequence time-series forecasting. In *Proceedings of the AAAI conference on artificial intelligence*, volume 35, pages 11106–11115, 2021.
- [4] Kaifeng Bi, Lingxi Xie, Hengheng Zhang, Xin Chen, Xiaotao Gu, and Qi Tian. Accurate medium-range global weather forecasting with 3d neural networks. *Nature*, 619(7970):533–538, 2023.
- [5] Shengchao Chen, Guodong Long, Jing Jiang, Dikai Liu, and Chengqi Zhang. Foundation models for weather and climate data understanding: A comprehensive survey. *arXiv preprint arXiv:2312.03014*, 2023.
- [6] Yuqi Nie, Nam H Nguyen, Phanwadee Sinthong, and Jayant Kalagnanam. A time series is worth 64 words: Long-term forecasting with transformers. *arXiv preprint arXiv:2211.14730*, 2022.
- [7] Brendan McMahan, Eider Moore, Daniel Ramage, Seth Hampson, and Blaise Aguera y Arcas. Communication-efficient learning of deep networks from decentralized data. In *Artificial intelligence and statistics*, pages 1273–1282. PMLR, 2017.
- [8] Xiaoxiao Li, Meirui Jiang, Xiaofei Zhang, Michael Kamp, and Qi Dou. Fedbn: Federated learning on non-iid features via local batch normalization. *arXiv preprint arXiv:2102.07623*, 2021.
- [9] Alysa Ziyang Tan, Han Yu, Lizhen Cui, and Qiang Yang. Towards personalized federated learning. *IEEE Transactions on Neural Networks and Learning Systems*, 2022.

- [10] Defu Cao, Furong Jia, Serkan O Arik, Tomas Pfister, Yixiang Zheng, Wen Ye, and Yan Liu. Tempo: Prompt-based generative pre-trained transformer for time series forecasting. *arXiv preprint arXiv:2310.04948*, 2023.
- [11] Ming Jin, Shiyu Wang, Lintao Ma, Zhixuan Chu, James Y Zhang, Xiaoming Shi, Pin-Yu Chen, Yuxuan Liang, Yuan-Fang Li, Shirui Pan, et al. Time-llm: Time series forecasting by reprogramming large language models. *arXiv preprint arXiv:2310.01728*, 2023.
- [12] Hans Hersbach, Bill Bell, Paul Berrisford, Shoji Hirahara, András Horányi, Joaquín Muñoz-Sabater, Julien Nicolas, Carole Peubey, Raluca Radu, Dinand Schepers, et al. The era5 global reanalysis. *Quarterly Journal of the Royal Meteorological Society*, 146(730):1999–2049, 2020.
- [13] Stephan Rasp, Peter D Dueben, Sebastian Scher, Jonathan A Weyn, Soukayna Moutadid, and Nils Thuerey. Weatherbench: a benchmark data set for data-driven weather forecasting. *Journal of Advances in Modeling Earth Systems*, 12(11):e2020MS002203, 2020.
- [14] Peter Bauer, Alan Thorpe, and Gilbert Brunet. The quiet revolution of numerical weather prediction. *Nature*, 525(7567):47–55, 2015.
- [15] Alec Radford, Jeffrey Wu, Rewon Child, David Luan, Dario Amodei, Ilya Sutskever, et al. Language models are unsupervised multitask learners. *OpenAI blog*, 1(8):9, 2019.
- [16] Hao Xue and Flora D Salim. Promptcast: A new prompt-based learning paradigm for time series forecasting. *IEEE Transactions on Knowledge and Data Engineering*, 2023.
- [17] Tian Zhou, Peisong Niu, Xue Wang, Liang Sun, and Rong Jin. One fits all: Universal time series analysis by pretrained lm and specially designed adaptors. *arXiv preprint arXiv:2311.14782*, 2023.
- [18] Ching Chang, Wen-Chih Peng, and Tien-Fu Chen. Llm4ts: Two-stage fine-tuning for time-series forecasting with pre-trained llms. *arXiv preprint arXiv:2308.08469*, 2023.
- [19] Edward J Hu, Yelong Shen, Phillip Wallis, Zeyuan Allen-Zhu, Yuanzhi Li, Shean Wang, Lu Wang, and Weizhu Chen. Lora: Low-rank adaptation of large language models. *arXiv preprint arXiv:2106.09685*, 2021.
- [20] Qingsong Wen, Tian Zhou, Chaoli Zhang, Weiqi Chen, Ziqing Ma, Junchi Yan, and Liang Sun. Transformers in time series: A survey. *arXiv preprint arXiv:2202.07125*, 2022.
- [21] Nikita Kitaev, Łukasz Kaiser, and Anselm Levskaya. Reformer: The efficient transformer. *arXiv preprint arXiv:2001.04451*, 2020.
- [22] Shizhan Liu, Hang Yu, Cong Liao, Jianguo Li, Weiyao Lin, Alex X Liu, and Schahram Dustdar. Pyraformer: Low-complexity pyramidal attention for long-range time series modeling and forecasting. In *International conference on learning representations*, 2021.
- [23] Yong Liu, Tengge Hu, Haoran Zhang, Haixu Wu, Shiyu Wang, Lintao Ma, and Mingsheng Long. itransformer: Inverted transformers are effective for time series forecasting. *arXiv preprint arXiv:2310.06625*, 2023.
- [24] Ailing Zeng, Muxi Chen, Lei Zhang, and Qiang Xu. Are transformers effective for time series forecasting? In *Proceedings of the AAAI conference on artificial intelligence*, volume 37, pages 11121–11128, 2023.
- [25] David Campos, Miao Zhang, Bin Yang, Tung Kieu, Chenjuan Guo, and Christian S Jensen. Lightts: Lightweight time series classification with adaptive ensemble distillation. *Proceedings of the ACM on Management of Data*, 1(2):1–27, 2023.
- [26] Xin Liu, Daniel McDuff, Geza Kovacs, Isaac Galatzer-Levy, Jacob Sunshine, Jiening Zhan, Ming-Zher Poh, Shun Liao, Paolo Di Achille, and Shwetak Patel. Large language models are few-shot health learners. *arXiv preprint arXiv:2305.15525*, 2023.
- [27] Shengchao Chen, Guodong Long, Tao Shen, Tianyi Zhou, and Jing Jiang. Spatial-temporal prompt learning for federated weather forecasting. *arXiv preprint arXiv:2305.14244*, 2023.
- [28] Shengchao Chen, Ting Shu, Huan Zhao, Qilin Wan, Jincan Huang, and Cailing Li. Dynamic multiscale fusion generative adversarial network for radar image extrapolation. *IEEE Transactions on Geoscience and Remote Sensing*, 60:1–11, 2022.
- [29] Shengchao Chen, Ting Shu, Huan Zhao, Guo Zhong, and Xunlai Chen. Tempee: Temporal-spatial parallel transformer for radar echo extrapolation beyond auto-regression. *IEEE Transactions on Geoscience and Remote Sensing*, 2023.
- [30] Xin Man, Chenghong Zhang, Jin Feng, Changyu Li, and Jie Shao. W-mae: Pre-trained weather model with masked autoencoder for multi-variable weather forecasting. *arXiv preprint arXiv:2304.08754*, 2023.
- [31] Remi Lam, Alvaro Sanchez-Gonzalez, Matthew Willson, Peter Wirnsberger, Meire Fortunato, Ferran Alet, Suman Ravuri, Timo Ewalds, Zach Eaton-Rosen, Weihua Hu, et al. Graphcast: Learning skillful medium-range global weather forecasting. *arXiv preprint arXiv:2212.12794*, 2022.

- [32] Sojung An, Junha Lee, Jiyeon Jang, Inchaee Na, Wooyeon Park, and Sujeong You. Self-supervised pre-training for precipitation post-processor. *arXiv preprint arXiv:2310.20187*, 2023.
- [33] Filip Hanzely, Slavomír Hanzely, Samuel Horváth, and Peter Richtárik. Lower bounds and optimal algorithms for personalized federated learning. *Advances in Neural Information Processing Systems*, 33:2304–2315, 2020.
- [34] Tian Li, Shengyuan Hu, Ahmad Beirami, and Virginia Smith. Ditto: Fair and robust federated learning through personalization. In *International Conference on Machine Learning*, pages 6357–6368. PMLR, 2021.
- [35] Tian Li, Anit Kumar Sahu, Manzil Zaheer, Maziar Sanjabi, Ameet Talwalkar, and Virginia Smith. Federated optimization in heterogeneous networks. *Proceedings of Machine learning and systems*, 2:429–450, 2020.
- [36] Liam Collins, Hamed Hassani, Aryan Mokhtari, and Sanjay Shakkottai. Exploiting shared representations for personalized federated learning. In *International conference on machine learning*, pages 2089–2099. PMLR, 2021.
- [37] Michael Zhang, Karan Sapra, Sanja Fidler, Serena Yeung, and Jose M Alvarez. Personalized federated learning with first order model optimization. *arXiv preprint arXiv:2012.08565*, 2020.
- [38] Alireza Fallah, Aryan Mokhtari, and Asuman Ozdaglar. Personalized federated learning with theoretical guarantees: A model-agnostic meta-learning approach. *Advances in Neural Information Processing Systems*, 33:3557–3568, 2020.
- [39] Ashish Vaswani, Noam Shazeer, Niki Parmar, Jakob Uszkoreit, Llion Jones, Aidan N Gomez, Łukasz Kaiser, and Illia Polosukhin. Attention is all you need. *Advances in neural information processing systems*, 30, 2017.
- [40] Haixu Wu, Jiehui Xu, Jianmin Wang, and Mingsheng Long. Autoformer: Decomposition transformers with auto-correlation for long-term series forecasting. *Advances in Neural Information Processing Systems*, 34:22419–22430, 2021.
- [41] Tian Zhou, Ziqing Ma, Qingsong Wen, Xue Wang, Liang Sun, and Rong Jin. Fedformer: Frequency enhanced decomposed transformer for long-term series forecasting. In *International Conference on Machine Learning*, pages 27268–27286. PMLR, 2022.
- [42] Gerald Woo, Chenghao Liu, Doyen Sahoo, Akshat Kumar, and Steven Hoi. Etsformer: Exponential smoothing transformers for time-series forecasting. *arXiv preprint arXiv:2202.01381*, 2022.
- [43] Tianping Zhang, Yizhuo Zhang, Wei Cao, Jiang Bian, Xiaohan Yi, Shun Zheng, and Jian Li. Less is more: Fast multivariate time series forecasting with light sampling-oriented mlp structures, 2022.
- [44] Jacob Devlin, Ming-Wei Chang, Kenton Lee, and Kristina Toutanova. Bert: Pre-training of deep bidirectional transformers for language understanding. *arXiv preprint arXiv:1810.04805*, 2018.
- [45] Hugo Touvron, Thibaut Lavril, Gautier Izacard, Xavier Martinet, Marie-Anne Lachaux, Timothée Lacroix, Baptiste Rozière, Naman Goyal, Eric Hambro, Faisal Azhar, et al. Llama: Open and efficient foundation language models. *arXiv preprint arXiv:2302.13971*, 2023.
- [46] Taesung Kim, Jinhee Kim, Yunwon Tae, Cheonbok Park, Jang-Ho Choi, and Jaegul Choo. Reversible instance normalization for accurate time-series forecasting against distribution shift. In *International Conference on Learning Representations*, 2021.
- [47] Yue Tan, Guodong Long, Lu Liu, Tianyi Zhou, Qinghua Lu, Jing Jiang, and Chengqi Zhang. Fedproto: Federated prototype learning across heterogeneous clients. In *Proceedings of the AAAI Conference on Artificial Intelligence*, volume 36, pages 8432–8440, 2022.
- [48] Shengchao Chen, Guodong Long, Tao Shen, and Jing Jiang. Prompt federated learning for weather forecasting: Toward foundation models on meteorological data. *arXiv preprint arXiv:2301.09152*, 2023.
- [49] Ilya Loshchilov and Frank Hutter. Decoupled weight decay regularization. *arXiv preprint arXiv:1711.05101*, 2017.
- [50] Jun Luo and Shandong Wu. Adapt to adaptation: Learning personalization for cross-silo federated learning. In *IJCAI: proceedings of the conference*, volume 2022, page 2166. NIH Public Access, 2022.
- [51] Manoj Ghuhana Arivazhagan, Vinay Aggarwal, Aaditya Kumar Singh, and Sunav Choudhary. Federated learning with personalization layers. *arXiv preprint arXiv:1912.00818*, 2019.
- [52] Jianqing Zhang, Yang Hua, Hao Wang, Tao Song, Zhengui Xue, Ruhui Ma, and Haibing Guan. Fedala: Adaptive local aggregation for personalized federated learning. In *Proceedings of the AAAI Conference on Artificial Intelligence*, volume 37, pages 11237–11244, 2023.
- [53] Chuhan Wu, Fangzhao Wu, Lingjuan Lyu, Yongfeng Huang, and Xing Xie. Communication-efficient federated learning via knowledge distillation. *Nature communications*, 13(1):2032, 2022.

- [54] Amirhossein Reisizadeh, Aryan Mokhtari, Hamed Hassani, Ali Jadbabaie, and Ramtin Pedarsani. Fedpaq: A communication-efficient federated learning method with periodic averaging and quantization. In *International conference on artificial intelligence and statistics*, pages 2021–2031. PMLR, 2020.
- [55] Zhuo Zhang, Yuanhang Yang, Yong Dai, Qifan Wang, Yue Yu, Lizhen Qu, and Zenglin Xu. Fedpetuning: When federated learning meets the parameter-efficient tuning methods of pre-trained language models. In *Annual Meeting of the Association of Computational Linguistics 2023*, pages 9963–9977. Association for Computational Linguistics (ACL), 2023.
- [56] Tao Guo, Song Guo, Junxiao Wang, Xueyang Tang, and Wenchao Xu. Promptfl: Let federated participants cooperatively learn prompts instead of models-federated learning in age of foundation model. *IEEE Transactions on Mobile Computing*, 2023.
- [57] Yang Cao, Haolong Xiang, Hang Zhang, Ye Zhu, and Kai Ming Ting. Anomaly detection based on isolation mechanisms: A survey. *arXiv preprint arXiv:2403.10802*, 2024.

APPENDIX: Personalized Adapter for Large Meteorology Model on Devices: Towards Weather Foundation Models

The appendix includes missing information from our main text, including: Appendix A More Related Work; Appendix B Experimental Details; Appendix C Theorems and Proof; Appendix D Additional Finding & Experiment & Discussion; Appendix E Full Experimental Results and Appendix F Additional Statements.

Appendix A More Related Work

In this section, we will discuss in detail advances relevant to our work, which include weather variable modeling, personalized federated learning, universal time series learning, and large language models (LLMs) in time series.

From Meteorological Variable Modeling to Weather Forecasting. Weather conditions play a crucial role in sectors such as transportation, tourism, and agriculture. Meteorological factors, including temperature, humidity, and precipitation, provide essential support and historical insights that enable researchers to analyze weather trends. For decades, Numerical Weather Prediction (NWP) [14] has been the prevalent method, employing physical models to simulate and forecast atmospheric dynamics. However, the accuracy of NWP can be compromised by the uncertainty of initial conditions in differential equations, particularly in complex atmospheric processes, and it requires significant computational resources [5, 27, 28, 29].

The recent exponential growth in weather data has prompted a shift from traditional physics-based methods to data-driven approaches using machine learning (ML) and deep learning (DL), which bypass physical constraints in meteorological variables [5]. DL strategies, with their deeper representational capabilities, generally surpass ML methods. Various deep network architectures have been employed to perform extensive weather modeling using large-scale reanalysis data [1, 4, 30, 31, 32]. Yet, these methods tend to focus on global weather patterns, often overlooking the specifics of regional weather variables, and thus fail to offer detailed regional analyses. Moreover, these models require extensive datasets and substantial computational resources—for example, some need to train on 192 NVIDIA Tesla V100 GPUs for 16 days [4]. Additionally, prevailing models assume centralized data storage, which contrasts with the decentralized data collection from diverse ground weather stations. Our research addresses these challenges by focusing on regional meteorological variables in low-resource settings, aiming to provide reliable analytical support for weather pattern modeling and understanding.

Personalized Federated Learning. Federated learning (FL) [7] is a distributed learning paradigm that facilitates the collaborative training of models without exposing data from each participant. Personalized FL (PFL) aims to train a personalized model for each client. Existing PFLs are based on various techniques. Refs. [33, 34, 35] add a regularization term that benefits decomposing the personalized model optimization from global model learning. Refs. [8, 36] share part of the model and keep personalized layers private to achieve personalization. Ref. [37] enables a more flexible personalization by adaptive weighted aggregation. Ref. [38] study PFL from a Model-Agnostic Meta-Learning where a meta-model is learned to generate the initialized local model for each client. This paper tackles on-device meteorological variable modeling from PFL perspective.

Universal Time Series Learning. On-device meteorological variable modeling addresses time series analysis of complex weather patterns on diverse, low-resource devices. We have expanded this to include task-specific time series learning. Recent advancements have enhanced Transformer [39] for time series forecasting by integrating signal processing techniques such as patching [6], exponential smoothing [40], decomposition [24], and frequency analysis [41]. Among them, PatchTST [6] improves the accuracy of long-term forecasting compared to other Transformer models. ETSFormer [42] applies principles of power series smoothing within the Transformer framework to boost efficiency. Similarly, FEDformer [41] merges the Transformer with seasonal & trend decomposition, offering improved performance and efficiency. Autoformer [40] leverages sequence periodicity for better dependency discovery and representation, excelling in both efficiency and accuracy.

While these methods excel in efficiency and accuracy, they are typically tailored for narrow-range forecasting on select classical time series datasets. Real-world weather data, however, often displays more complex patterns and interconnected variable relationships. Furthermore, weather modeling extends beyond forecasting, rendering these methods less effective for weather sequences. To improve modeling for intricate weather sequences, models need the flexibility to adjust to complex distributions and various tasks with minimal training. The ideal weather models would capture weather patterns accurately, facilitating knowledge transfer, such as between regions. However, creating versatile weather models remains a challenging endeavor. Recent studies have started to examine the potential of large-scale climate models [1, 4], utilizing simulated datasets advances. Yet, their generalizability is hindered by data differences, complex architectures, and the vast number of model parameters.

LLMs in Time Series. Large language models (LLMs) have spurred advances in natural language processing (NLP). Although time series modeling hasn't seen similar leaps, the impressive capabilities of LLMs have led to their use in this field. In general, pre-trained LLMs are often fine-tuned or reprogrammed to model

time series [18, 11, 10, 17]. Among them, PROMPTCAST [16] and HEALTHLEARNER [26] treat time series as "text sequences," inputting them directly into LLMs and using prompts for forecasting. [17] decodes time series as embeddings for LLM output, showing LLMs' strength in time series analysis. LLM4TS [18] uses a two-stage fine-tuning approach to adapt LLMs to time series data. TEMPO [10] breaks down time series features to leverage LLMs in prediction tasks, while TIME-LLM [11] fine-tunes LLMs with multimodal data, integrating relevant text prompts for efficient analysis. However, these approaches focus on centralized time series modeling and overlook the complexities of real-world distributed settings. Weather data, in particular, has unique challenges like heterogeneity from geographic factors and privacy concerns, making central training methods both risky and difficult.

Appendix B Experimental Details

B.1 Datasets

Despite the proliferation of reanalysis data aimed at building frameworks for global climate analysis, these datasets often struggle to model regional weather trend due to: (1) they depend on numerous simulations of atmospheric equations, introducing biases inconsistent with real observations, and (2) they face challenges in refining their scale to suit specific regional applications. Hence, we collected real observational data from various weather stations across different regions. We then organized this data into two series, each comprising two distinct datasets, to underscore the heterogeneity inherent in real-world settings.

On-device Weather Series 1# (ODW1). The dataset gathered from 15 ground weather stations across China, Japan, and South Korea, encompasses over 20 variables. It has been divided into two subsets: **ODW1T** has a heterogeneous time span, meaning the data collection start and end times vary by location. and **ODW1V** extends **ODW1T** by adding variability in the observed variables; while one variable remains constant at each station, the others vary. The temporal resolution of the dataset is 1h. Details are presented in **Tab. 8** and **Tab. 9**.

Table 8: Details about **ODW1T** dataset, where **Start** and **End** indicate the respective beginning and ending timestamps of data collected at a specific weather station, **Samples** denotes the count of weather sequence samples gathered at that station, and **Variables** refers to the weather variables included in the data from each station (For the full names of these variables, please refer to **Tab. 12**).

Weather Station	Start (UTC+0)	End (UTC+0)	Num. of Samples #	Variables
Hua-Nan	06/11/2018 16:00	03/19/2020 00:00	230,280	ap, t, mxt, mnt, dt, rh, wvp, p1, p2, p3, p4, p5, wd, ws, mwd, mws, st, hv1, hv2, vv
E-Min	01/23/2019 16:00	06/07/2024 04:00	240,280	
Huhehaote	09/02/1028 01:00	06/01/2020 07:00	306,400	
Yin-Chuan	10/31/2018 20:00	05/06/2020 07:00	265,220	
Shen-Yang	04/09/2018 01:00	08/30/2019 06:00	243,980	
Hai-Dian	05/29/2017 16:00	12/05/2018 11:00	266,340	
Xin-Du	01/29/2020 08:00	06/29/2021 00:00	248,040	
Lin-Zhi	10/13/2019 08:00	03/30/2021 09:00	256,380	
Kun-Ming	08/28/2018 07:00	06/13/2020 22:00	314,740	
Wu-Han	05/20/2019 01:00	02/17/2021 21:00	247,160	
Tokyo	07/17/2017 23:00	01/27/2019 14:00	248,180	
Nagoya	05/10/2017 15:00	02/14/2019 17:00	309,680	
Hiroshima	05/27/2019 10:00	11/01/2020 03:00	251,420	
Seoul	04/28/2017 04:00	11/20/2018 00:00	274,040	
Busan	02/24/1029 18:00	07/17/2020 17:00	244,340	

On-device Weather Series 2# (ODW2). This dataset consists of data from 36 weather observation stations in the United States, Canada, and Israel, covering 5 different variables with a temporal resolution of 1 hour. Following the dataset setting of **ODW1**, the dataset was also subdivided into two different dataset, including **ODW2T** and **ODW2V**. Detailed information are presented in **Tab. 10** and **Tab. 11**.

Remark. Four standard steps were performed during the collection and compilation of these dataset, as shown below:

- [1] **Collection of Raw Meteorological Data.** Raw data collection represents the foundational and initial step in constructing our dataset. We procure open-source raw data from various national meteorological centers and data repositories, including the National Meteorological Science Data Center of China¹, Korea Meteorological Administration², Global Surface Meteorological Observations Historical Dataset³, Canadian Meteorological Data Center⁴, and World Weather Data Repository

¹<https://data.cma.cn/>

²<https://www.kma.go.kr/>

³<https://k.data.cma.cn/mekb/?r=dataService/cdcindex&datacode=A.0020.0002.S001>

⁴<https://weather.gc.ca/>

Table 9: Details about **ODW1V** dataset, where **Start** and **End** indicate the respective beginning and ending timestamps of data collected at a specific weather station, **Num. of Samples #** denotes the count of weather sequence samples gathered at that station, and **Fixed Variables** refers to the shared variables among different weather stations, and **Other Variables** is the remain weather variables in each weather station (For the full names of these variables, please refer to **Tab. 12**).

Weather Station	Start (UTC+0)	End (UTC+0)	Num. of Samples #	Fixed Variable	Other Variables
Hua-Nan	06/11/2018 16:00	03/19/2020 00:00	69,084	Temperature	ws, p4, p1, p5, p2
E-Min	01/23/2019 16:00	06/07/2024 04:00	72,072		p1, mwd, p2, wvp, ws
Huhehaote	09/02/1028 01:00	06/01/2020 07:00	91,920		vv, p3, dt, mwd, p4
Yin-Chuan	10/31/2018 20:00	05/06/2020 07:00	79,566		ws, dt, mnt, p3, p2
Shen-Yang	04/09/2018 01:00	08/30/2019 06:00	73,194		wd, st, hv1, mwd, vv
Hai-Dian	05/29/2017 16:00	12/05/2018 11:00	79,902		p5, rh, ap, mxt, mwd
Xin-Du	01/29/2020 08:00	06/29/2021 00:00	74,412		p1, hv1, wvp, mxt, p5
Lin-Zhi	10/13/2019 08:00	03/30/2021 09:00	76,914		ws, vv, p1, hv1, p5
Kun-Ming	08/28/2018 07:00	06/13/2020 22:00	94,422		hv2, mws, mnt, p2, mwd
Wu-Han	05/20/2019 01:00	02/17/2021 21:00	92,148		st, ws, p3, p5, rh
Tokyo	07/17/2017 23:00	01/27/2019 14:00	80,454		p5, st, hv1, ws, hv2
Nagoya	05/10/2017 15:00	02/14/2019 17:00	92,904		mwd, p1, mws, mnt, st
Hiroshima	05/27/2019 10:00	11/01/2020 03:00	75,426		p4, mwd, wd, hv1, dt
Seoul	04/28/2017 04:00	11/20/2018 00:00	82,212		hv1, mwd, vv, rh, p4
Busan	02/24/1029 18:00	07/17/2020 17:00	73,302		p4, p3, wvp, p1, vv

Table 10: Details about **ODW2T** dataset, where **Start** and **End** indicate the respective beginning and ending timestamps of data collected at a specific weather station, **Num. of Samples #** denotes the count of weather sequence samples gathered at that station, and **Variables** refers to the weather variables included in the data from each station (For meaning of variables, please refer to **Tab. 12**).

Weather Station	Start (UTC+0)	End (UTC+0)	Num. of Samples #	Variables
Albuquerque	02/26/2016 01:00	11/16/2016 19:00	31,780	h, p, t, wd, ws
Atlanta	03/24/2013 21:00	12/05/2013 18:00	30,715	
Beersheba	05/06/2014 06:00	03/26/2015 18:00	35,350	
Boston	04/06/2015 10:00	03/23/2016 00:00	35,120	
Charlotte	08/10/2013 09:00	04/24/2014 14:00	30,875	
Chicago	06/09/2015 17:00	03/22/2016 10:00	34,415	
Dallas	04/11/2013 00:00	08/26/2014 11:00	35,463	
Denver	06/23/2015 22:00	05/18/2016 02:00	39,510	
Detroit	10/30/2012 06:00	08/22/2013 22:00	35,610	
Eilat	11/24/2012 19:00	08/02/2013 05:00	30,060	
Haifa	05/18/2013 21:00	04/16/2014 14:00	39,915	
Houston	12/19/2013 02:00	11/13/2014 02:00	39,490	
Indianapoils	01/10/2016 23:00	10/07/2016 04:00	32,435	
Jacksonville	11/11/2012 16:00	09/28/2013 01:00	38,455	
Jerusalem	04/22/2015 03:00	02/28/2016 01:00	37,440	
Kansas City	06/03/2015 12:00	03/08/2016 21:00	33,535	
Las Vegas	11/25/2014 09:00	10/19/2015 15:00	39,400	
Los Angeles	07/04/2013 08:00	04/28/2014 18:00	35,820	
Miami	02/10/2014 10:00	12/05/2014 10:00	35,770	
Minneapolis	10/17/2013 03:00	08/31/2014 15:00	38,230	
Montreal	08/14/2015 07:00	04/26/2016 06:00	30,725	
Nahariyya	12/03/2013 02:00	09/18/2014 01:00	34,685	
Nashville	02/08/2017 03:00	11/13/2017 15:00	33,430	
New York	09/27/2013 20:00	06/14/2014 15:00	31,185	
Philadelphia	12/08/2012 05:00	09/13/2013 20:00	33,565	
Phoenix	07/25/2013 15:00	06/05/2014 09:00	37,780	
Pittsburgh	10/16/2015 06:00	07/19/2016 16:00	33,300	
Portland	10/12/2013 12:00	06/27/2014 18:00	31,000	
Saint Louis	09/16/2014 13:00	07/21/2015 06:00	36,935	
San Antonio	03/15/2014 01:00	12/03/2014 20:00	31,665	
San Diego	07/02/2015 11:00	03/18/2016 00:00	31,155	
San Francisco	05/10/2013 06:00	01/21/2014 12:00	30,760	
Seattle	08/06/2014 22:00	06/28/2015 05:00	39,045	
Tel Aviv District	09/23/2013 06:00	06/27/2014 18:00	33,310	
Toronto	12/06/2016 16:00	10/19/2017 15:00	38,045	
Vancouver	08/26/2015 10:00	06/02/2016 20:00	33,780	

from Kaggle⁵. This process ensures that the collected weather data from these sources are consistent

⁵<https://www.kaggle.com/datasets>

Table 11: Details about **ODW2V** dataset, where **Start** and **End** indicate the respective beginning and ending timestamps of data collected at a specific weather station, **Num. of Samples #** denotes the count of weather sequence samples gathered at that station, and **Fixed Variables** refers to the shared variables among different weather stations, and **Other Variables** is the remain weather variables in each weather station (For the full names of these variables, please refer to **Tab. 12**).

Weather Station	Start (UTC+0)	End (UTC+0)	Num. of Samples #	Fixed Variable	Other Variables
Albuquerque	02/26/2016 01:00	11/16/2016 19:00	19,068	Humidity	ws, wd
Atlanta	03/24/2013 21:00	12/05/2013 18:00	18,429		wd,p
Beersheba	05/06/2014 06:00	03/26/2015 18:00	21,210		t, ws
Boston	04/06/2015 10:00	03/23/2016 00:00	21,072		ws, wd
Charlotte	08/10/2013 09:00	04/24/2014 14:00	18,525		t, p
Chicago	06/09/2015 17:00	03/22/2016 10:00	20,649		t, p
Dallas	04/11/2013 00:00	08/26/2014 11:00	21,279		p, wd
Denver	06/23/2015 22:00	05/18/2016 02:00	23,706		t, p
Detroit	10/30/2012 06:00	08/22/2013 22:00	21,366		p, t
Eilat	11/24/2012 19:00	08/02/2013 05:00	18,036		ws, p
Haifa	05/18/2013 21:00	04/16/2014 14:00	23,949		ws, t
Houston	12/19/2013 02:00	11/13/2014 02:00	23,694		p, wd
Indianapolis	01/10/2016 23:00	10/07/2016 04:00	19,461		t, p
Jacksonville	11/11/2012 16:00	09/28/2013 01:00	23,073		ws, t
Jerusalem	04/22/2015 03:00	02/28/2016 01:00	22,464		ws, p
Kansas City	06/03/2015 12:00	03/08/2016 21:00	20,121		wd, ws
Las Vegas	11/25/2014 09:00	10/19/2015 15:00	23,640		p, t
Los Angeles	07/04/2013 08:00	04/28/2014 18:00	21,492		ws, t
Miami	02/10/2014 10:00	12/05/2014 10:00	21,462		wd, ws
Minneapolis	10/17/2013 03:00	08/31/2014 15:00	22,938		t, p
Montreal	08/14/2015 07:00	04/26/2016 06:00	18,435		wd, p
Nahariyya	12/03/2013 02:00	09/18/2014 01:00	20,811		p, ws
Nashville	02/08/2017 03:00	11/13/2017 15:00	20,058		wd, ws
New York	09/27/2013 20:00	06/14/2014 15:00	18,711		t, p
Philadelphia	12/08/2012 05:00	09/13/2013 20:00	20,139		ws, wd, h
Phoenix	07/25/2013 15:00	06/05/2014 09:00	22,668		ws, wd
Pittsburgh	10/16/2015 06:00	07/19/2016 16:00	19,980		wd, ws
Portland	10/12/2013 12:00	06/27/2014 18:00	18,600		ws, p
Saint Louis	09/16/2014 13:00	07/21/2015 06:00	22,161		t, wd
San Antonio	03/15/2014 01:00	12/03/2014 20:00	18,999		t, wd
San Diego	07/02/2015 11:00	03/18/2016 00:00	18,693		t, p
San Francisco	05/10/2013 06:00	01/21/2014 12:00	18,456		p, t
Seattle	08/06/2014 22:00	06/28/2015 05:00	23,427	t, wd	
Tel Aviv District	09/23/2013 06:00	06/27/2014 18:00	19,986	t, p	
Toronto	12/06/2016 16:00	10/19/2017 15:00	22,827	wd, p	
Vancouver	08/26/2015 10:00	06/02/2016 20:00	20,268	wd, ws	

in terms of temporal resolution and variable dimensions. All raw data are open-source and can be freely utilized or modified.

- [2] **Selection of Critical Meteorological Variables.** To support personalized on-device meteorological variable modeling and enhance regional weather forecasting reliability, we selected twenty representative meteorological variables. These variables, including temperature, barometric pressure, relative humidity, and precipitation, were chosen based on their significant impact on weather conditions. Detailed definitions, physical descriptions, and units of these selected variables are provided in **Table 12**.
- [3] **Ensuring Completion of Meteorological Time Series.** In this step, we primarily focus on ensuring the completeness of weather time series data collected from ground weather stations. Incomplete weather time series can generate unreliable predictions, potentially leading to significant unforeseen losses. Most ground weather stations are susceptible to unpredictable events such as power outages and equipment damage, which may result in data gaps. To enhance dataset completeness, we meticulously examined the raw data for missing values across various timestamps and employed a linear interpolation strategy to fill these gaps.
- [4] **Handling of Outliers.** Outliers are common in weather time series data. We distinguish between factual outliers, typically caused by extreme weather events (e.g., heavy rainfall, typhoons, thunderstorms), and non-factual outliers, often due to observational device anomalies or sensor malfunctions at weather stations. We identify significant deviations in a weather variable—for instance, a sudden increase from an average rainfall of 2 mm to 200 mm—as outliers. These are manually corrected; initially, the values are set to zero and then replaced using linear interpolation, reflecting the gradual nature of weather phenomena.

Table 12: Abbreviations, full names and corresponding units of the different variables in our proposed datasets.

Abbreviation	Full name	Unit
ap	Air Pressure	<i>hpa</i>
t	Air Temperature	$^{\circ}C$
mxt	Maximum Temperature	$^{\circ}C$
mnt	Minimum Temperature	$^{\circ}C$
dt	Dewpoint Temperature	$^{\circ}C$
rh	Relative Humidity	%
wvp	Water Vapor Pressure	<i>hpa</i>
p1	Precipitation in 1h	<i>mm</i>
p2	Precipitation in 3h	<i>mm</i>
p3	Precipitation in 6h	<i>mm</i>
p4	Precipitation in 12h	<i>mm</i>
p5	Precipitation in 24h	<i>mm</i>
wd	Wind Direction	$^{\circ}C$
ws	Wind Speed	ms^{-1}
mwd	Maximum Wind Direction	$^{\circ}$
st	Land Surface Temperature	$^{\circ}C$
hv1	Horizontal Visibility in 1 min	<i>m</i>
hv2	Horizontal Visibility in 10 min	<i>m</i>
vv	Vertical Visibility	<i>m</i>

Visualisation. We hope to deepen the reader’s understanding of the datasets we have collected and compiled by providing standard visualizations. Considering the overall size of the datasets and the large number of meteorological variables, we have provided visualisations of representative variables here for reference. The visualisation of OWD1 is shown in Fig. 2. Due to the number of devices involved in the OWD2 dataset, we have divided it into two consecutive images for presentation, as shown in Fig 3 and Fig. 4.

B.2 Baselines

We compare with state-of-the-art time series analysis models and put them into Federated Learning environments, including Transformer-based methods like Transformer [39], Informer [3], Reformer [21], Pyraformer [22], iTransformer [23], and PatchTST [6], and recent competitive models including GPT4TS [17], DLinear [24] and LightTS [43], detailed information about baselines is below:

- **Transformer.** [39] This model uses a self-attention mechanism, popular for time series prediction tasks, to efficiently and accurately learn relationships within a sequence and contextual information.
- **Informer.** [3] An optimized Transformer-based model for long-range time series prediction. It uses ProbSparse self-attention for efficiency, processes long inputs effectively, and employs a fast prediction decoder.
- **Reformer.** [21] This model improves Transformer efficiency by using locality-sensitive hashing for attention and reversible residual layers. It offers better memory efficiency and speed for lengthy sequences without sacrificing performance.
- **Pyraformer.** [22] It features hierarchical pyramidal attention modules with binary trees to capture temporal dependencies across different ranges efficiently, both in time and memory complexity.
- **iTransformer.** [23] The iTransformer adds attention and feedforward networks to the inverse dimension. It embeds time points as variable tokens, using attention to capture multivariate correlations and feedforward networks for nonlinear representation of each token.
- **PatchTST.** [6] This method divides the time series into patches at the subseries level for input to the Transformer. Each channel holds a univariate time series, sharing the same embedding and Transformer weights across all series.
- **DLinear.** [24] DLinear integrates decomposition schemes from Autoformer and FEDformer with linear layers to model time series data tables. It effectively summarizes trend and seasonal components, enhancing performance on datasets rich in trends.
- **LightTS.** [43] A lightweight structure based on a simple MLP. It utilizes two downsampling strategies—spaced and sequential sampling—on the MLP structure, capitalizing on the fact that downsampled time series generally maintain most of their original information.

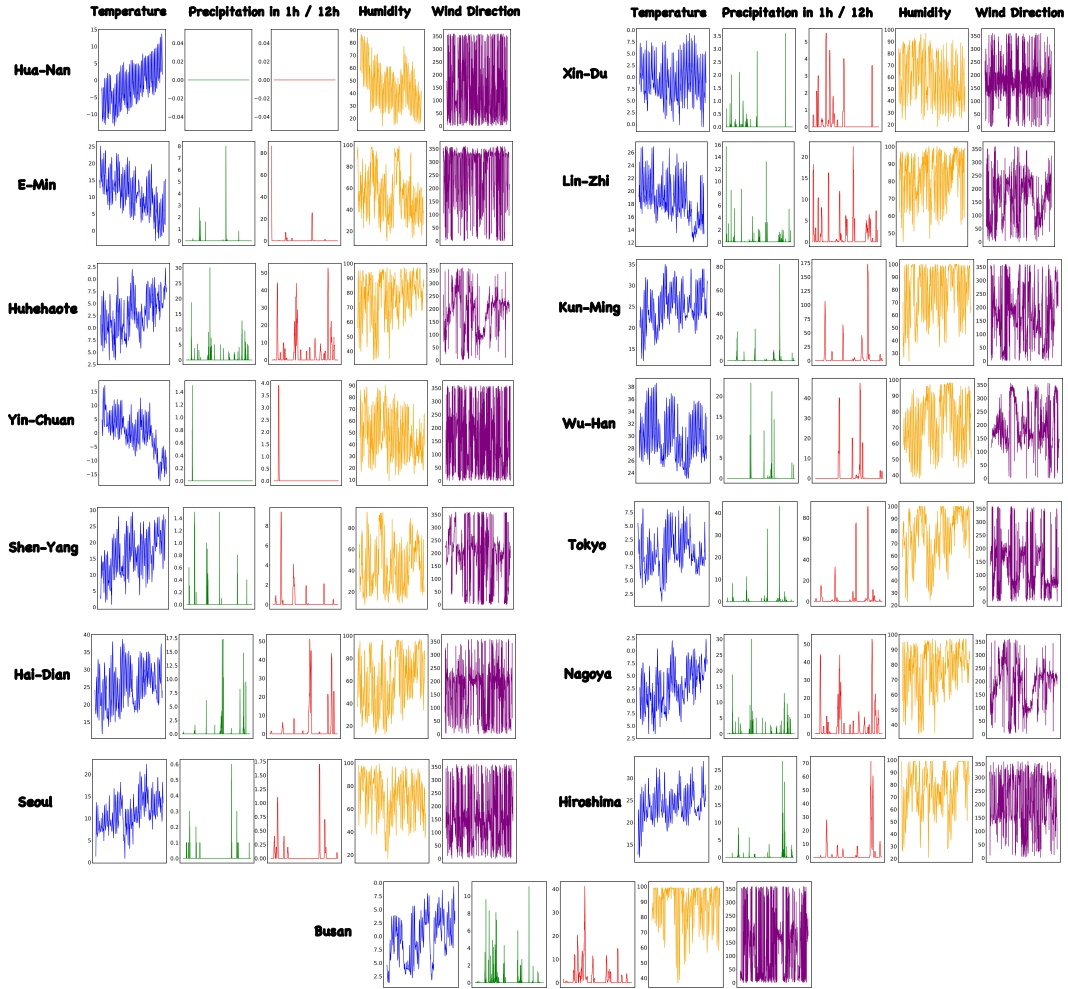


Figure 2: Visualisation of partial variables in ODW1 dataset, where we have selected the first 1,000 time points for presentation. The data distribution from different ground weather stations exhibit significant heterogeneity, and even though the trends of some variables may be similar, there are serious differences in magnitudes. The selected variables are, from left to right, temperature, precipitation in 1-hour/12-hour, humidity, and wind direction.

- **GPT4TS.** [17] This model is designed for time series analysis across various scenarios, achieved by fine-tuning a pre-trained language model, specifically GPT2, for the time series domain. It's important to note that for a fair comparison, our baseline setup differs from the original publication's configuration. Instead of using the first six layers of GPT2 as the backbone, we align with our approach and utilize only the first five layers.

In addition, pre-trained language models (PLMs) are the key component of our LM-Weather, we use different PLMs as the backbone to demonstrate the PLM can as the strong weather foundation model for on-device weather modeling. We use GPT-2 as the default setting, and BERT [44], LLaMA [45] as the alternatives.

- **BERT.** [44] BERT, short for Bidirectional Encoder Representations from Transformers, is a deep learning model that uses the Transformer architecture. It understands the context of words by analyzing text in both directions. When used as a baseline for evaluation, we only employ the first 5 layers of the pre-trained BERT.
- **GPT-2.** [15] Developed by OpenAI, GPT-2 is a language model that can generate coherent and diverse text based on a given prompt. In our research, we utilize the first 5 layers of the pre-trained GPT-2-base.
- **LLaMa.** [45] LLaMa stands for Large Language Model Meta AI and is a series of cutting-edge language models with sizes ranging from 7B to 65B parameters. They offer top-notch performance

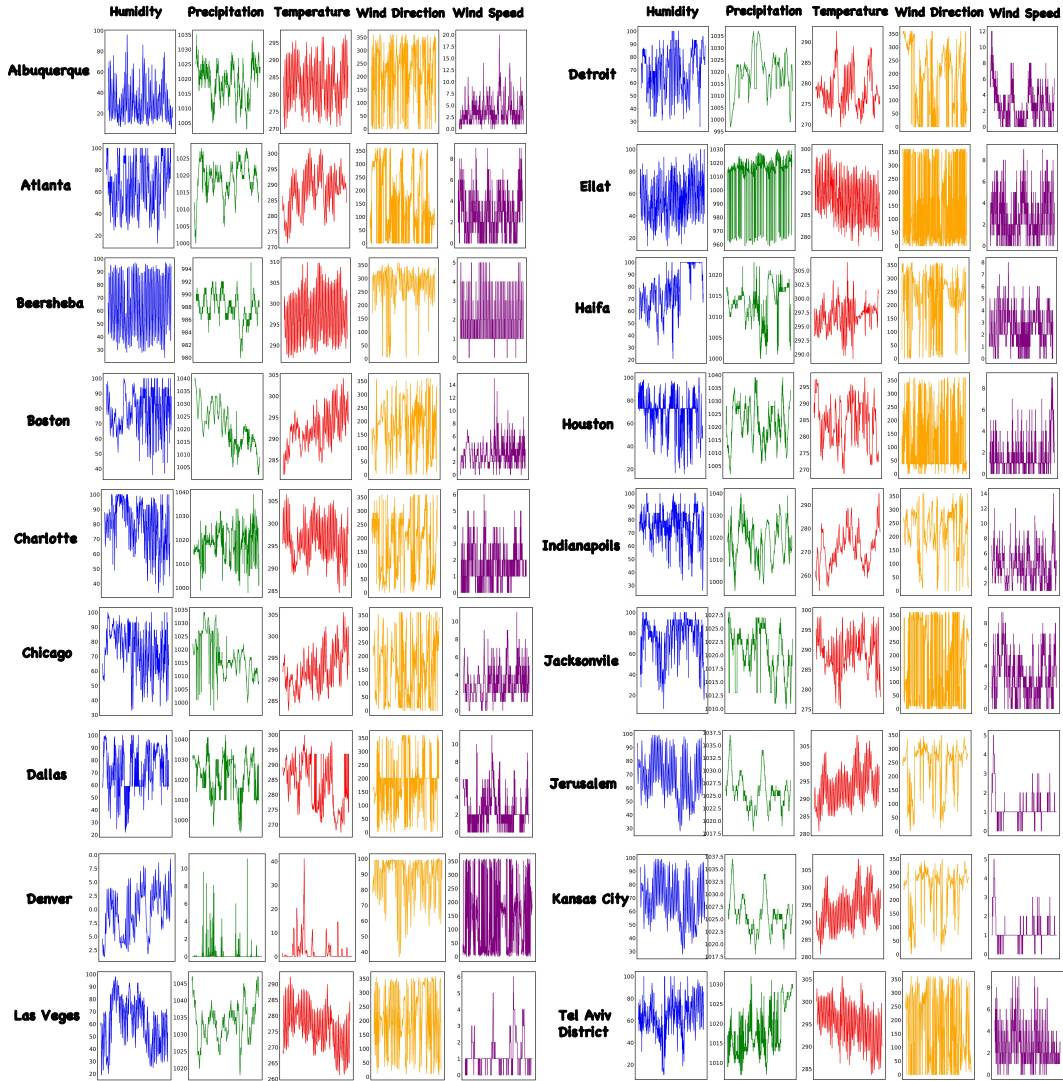


Figure 3: Visualisation of partial variables in ODW2 dataset, where we have selected the first 1,000 time points for presentation. The data distribution from different ground weather stations exhibit significant heterogeneity, and even though the trends of some variables may be similar, there are serious differences in magnitudes. The selected variables are, from left to right, humidity, precipitation, temperature, wind direction, and wind speed.

with less computational power and resources. In our research, we utilize the first 4 layers of the 3B LLaMa model.

B.3 Task Setups

We evaluate our proposed LM-WEATHER using four distinct on-device weather modeling datasets, each with tailored settings for various tasks. The specific task settings for these datasets are detailed in **Tab. 13**. Additionally, the specific tasks and scenarios for the on-device weather forecasting/imputation vary by dataset, as outlined in **Tab. 14**.

B.4 Implementation

We mainly follow the experimental configurations across all baselines within a unified evaluation pipeline in <https://github.com/thuml/Time-Series-Library> for fair comparison. Specially, we use GPT-2-base as the default backbone model unless state otherwise. All our experiments are repeat five times and we report

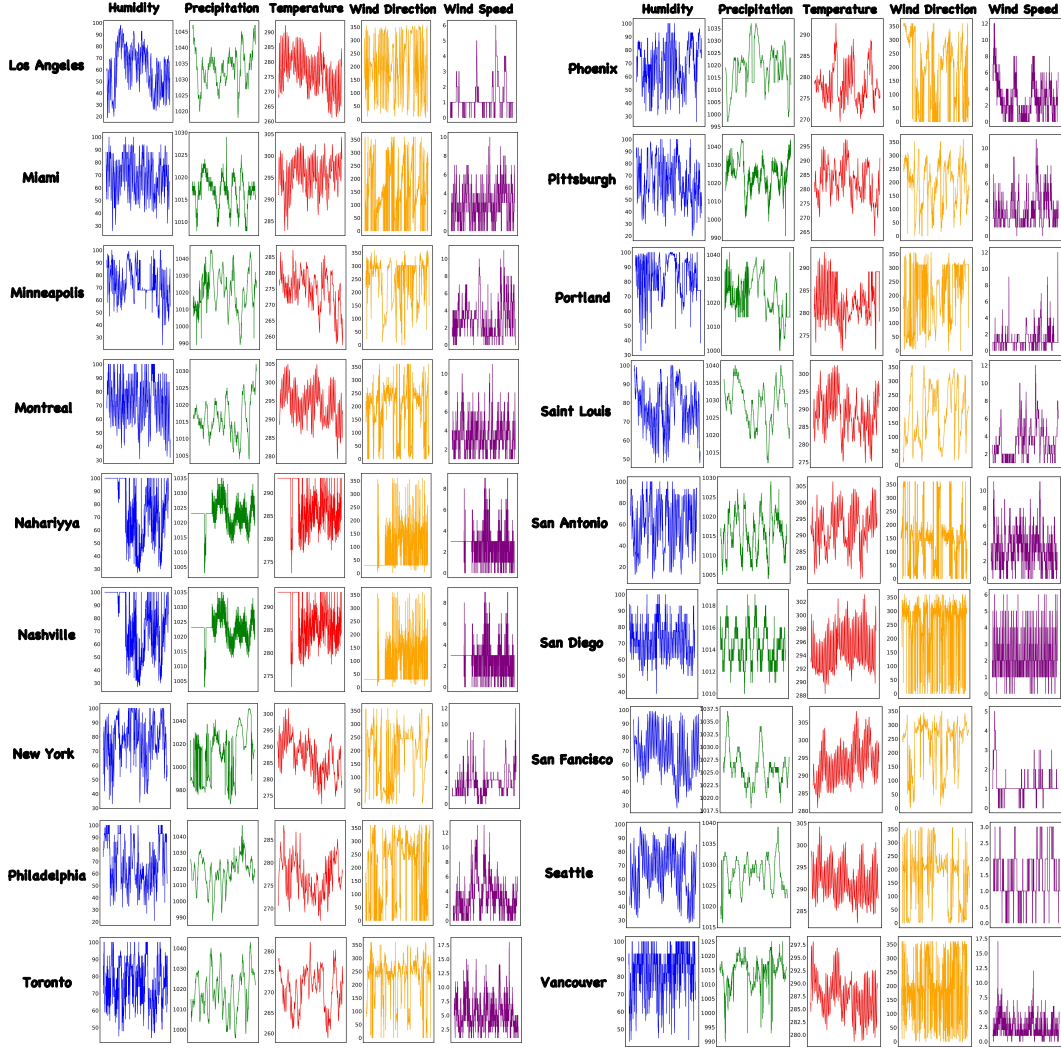


Figure 4: (**Figure 3** continued) Visualisation of partial variables in ODW2 dataset, where we have selected the first 1,000 time points for presentation. The selected variables are, from left to right, humidity, precipitation, temperature, wind direction, and wind speed.

Table 13: Task setup for different datasets during the evaluation. Note that for the imputation task there are actually no historical observations, but rather they are performed on a single long sequence.

Dataset	Task	Historical Observation Horizon	Prediction Horizon	Random Masking Ratio
ODW1T	Forecasting	192	{96, 192, 336, 720}	N
	Imputation	Consistent with the prediction horizon		{25%, 35%, 50%}
ODW1V	Forecasting	192		N
	Imputation	Consistent with the prediction horizon		{25%, 35%, 50%}
ODW2T	Forecasting	192		N
	Imputation	Consistent with the prediction horizon		{25%, 35%, 50%}
ODW2V	Forecasting	192		N
	Imputation	Consistent with the prediction horizon		{25%, 35%, 50%}

the averaged results. Our detailed model configurations are in Appendix B.8. All the algorithm implementations and designs in this study are based on Py torch and the algorithms are run on two RTX3090 GPUs 24GB.

Table 14: Summary of framework evaluation scenarios for various datasets. **Scenario 1/2/3/4** (in forecasting) refers to multivariate to univariate forecasting, where all historical variables are used to predict a single future variable. **All** represents multivariate to multivariate forecasting, meaning all variables predict all others. The symbol "-" indicates a non-existent scenario for that dataset. **Scenario 1/2/3** (in imputation) indicates different masking ratios for the original weather sequences.

Dataset	Forecasting					Imputation		
	Scenario 1	Scenario 2	Scenario 3	Scenario 4	Scenario 5	Scenario 1	Scenario 2	Scenario 3
ODW1T	Temperature	Humidity	Wind Speed	Surface Temperature	All			
ODW1V	Temperature	-	-	-	All			
ODW2T	Temperature	Humidity	-	-	All	25%	35%	50%
ODW2V	Humidity	-	-	-	All			

B.5 Technical Details

Reversible Normalization. In time series analysis, statistical properties like mean and variance often shift over time, indicating distributional changes in the data. To address this, we’ve incorporated Reversible Normalization (RevIn) [46] into our LM-WEATHER. Specifically, we’ve integrated RevIn into our Task Adapter Generation. This introduces two dynamic factors that adaptively normalize segments of the meteorological variable sequence \mathcal{X} , or their decomposed components (Trend $\mathcal{X}_{\text{Trend}}$, Seasonal $\mathcal{X}_{\text{Seasonal}}$, Residual $\mathcal{X}_{\text{Residual}}$), enhancing the accuracy of meteorological variable modeling. Specifically, for the trend component of \mathcal{X} , i.e., $\mathcal{X}_{\text{Trend}}$, its transformed value $\mathcal{X}'_{\text{Trend}}$ can be given by:

$$\mathcal{X}'_{\text{Trend}} = \gamma_T \left(\mathcal{X}_{\text{Trend}} - \frac{\mathbb{E}[\mathcal{X}_{\text{Trend}}]}{\sqrt{\text{Var}[\mathcal{X}_{\text{Trend}}] + \epsilon_T}} \right) + \beta_T \quad (6)$$

where $\mathbb{E}[\mathcal{X}_{\text{Trend}}]$ and $\text{Var}[\mathcal{X}_{\text{Trend}}]$ are the instance-specific mean and variance, respectively. γ_T and β_T are the trainable parameters for this component. This transformation is also applied to both the seasonal and residual components.

Pre-trained Language Model (PLM). In LM-WEATHER, we do not change the main architecture of the PLM, but use the parameter-efficient fine-tuning (PEFT) strategy to avoid large-scale parameter variations to ensure high efficiency on resource-constrained weather devices, and in this way, to achieve more reliable cross-domain knowledge transfer. Specifically, we introduce LoRA in the local PLM, which allows only **1.5%** of the PLM parameters to be trained while the rest remain frozen, as shown in Fig. Note that LoRA is only applied to the query and value of each Attention in the PLM, and the resulting low-rank matrices are used for global sharing between the client and the server.

Low-Rank Adaption (LoRA). To achieve more reliable cross-domain knowledge transfer (i.e., from natural language to complex weather sequences) while guaranteeing higher efficiency, we introduce LoRA [19], a parameter-efficient fine-tuning method for large language models, into PLM. Specifically, LoRA is applied to the *Query* and *Value* of each Attention layer by creating low-rank matrices for two pre-trained parameters W_q and W_k :

$$\text{QUERY} = W_q \mathcal{X} + A_q B_q, \quad \text{VALUE} = W_v \mathcal{X} + A_v B_v, \quad (7)$$

where \mathcal{X} denote the latent representation from input weather sequences through PLM’s word embedding layer. $A_q \in \mathbb{R}^{d \times r}$ and $B_q \in \mathbb{R}^{r \times d}$ are low-rank matrices created from $W_q \in \mathbb{R}^{d \times d}$, $A_v \in \mathbb{R}^{d \times r}$ and $B_v \in \mathbb{R}^{r \times d}$ are low-rank matrices created from $W_v \in \mathbb{R}^{d \times d}$, d is the number of dimensions, r is the rank, and $r \ll d$. It’s important to note that only the low-rank matrices A_q, B_q, A_v, B_v are trainable; the others remain fixed during training. Initially, A_q and A_v are set with random Gaussian values, and B_q and B_v start as zero at the beginning of training.

Task Adapter Generation. The $\mathcal{X}_{\text{Trend}}, \mathcal{X}_{\text{Seasonal}}, \mathcal{X}_{\text{Residual}}$ obtained from decomposition are used to generate *Task Adapter* via an unified generator as **Fig. 1B** that consisting of Token Embedding, Position Embedding, and Temporal Embedding. Specially, we use one-dimensional convolution operation to map each each specific sample $\mathcal{X}^k \in \mathbb{R}^{T \times 1}$ while keeping raw shape to generate TOKEN ADAPTER $\mathbf{P}_{\text{TO}} \in \mathbb{R}^{T \times C}$, as

$$\mathbf{P}_{\text{TO}}^k = \text{CONV1D}(\mathcal{X}^k), \quad \mathbf{P}_{\text{TO}} = \text{CONV1D}(\mathcal{X}) \quad (8)$$

Additionally, we use a trainable lookup table to map each point’s explicit position in the entire sequence, to generate POSITION ADAPTER $\mathbf{P}_{\text{PO}} \in \mathbb{R}^{T \times C}$, as:

$$\mathbf{P}_{\text{PO}} = \mathbf{E}(\text{INDEX}(\mathcal{X})), \quad (9)$$

where $\mathbf{E}(\cdot)$ is the trainable lookup table, and $\text{INDEX}(\cdot)$ is a function that achieve the indices of each point’s locations of weather sequence \mathcal{X} . Furthermore, we separately encode different time attributes such as minutes,

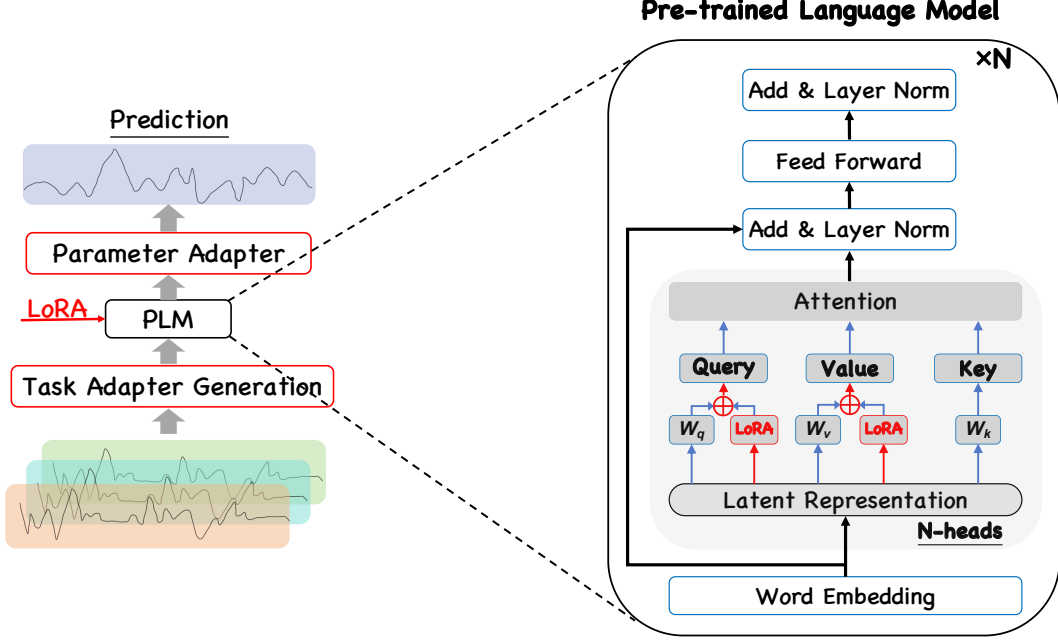


Figure 5: Schematic diagram of the PLM in LM-WEATHER, where we introduced LoRA to the PLM, to achieve more reliable cross-domain knowledge transfer while at the same time ensuring greater efficiency in adapting to low-resource weather devices.

hours, days, weeks, and months, using trainable parameters to dynamically model complex temporal shifts, to generate TEMPORAL ADAPTER P_{TE} , as

$$P_{TE} = \sum_{\alpha \in \{\text{mins, hours, days, weeks, months}\}} E_{\alpha}(\mathcal{X}) \quad (10)$$

where α represents different temporal attributes, E_{α} denotes the trainable lookup table for each temporal attributes. Finally, for each decomposition components, corresponding generated adapters can be obtained by aggregating Token Adapter $P_{TO} \in \mathbb{R}^{L \times C}$, Position Adapter $P_{PO} \in \mathbb{R}^{L \times C}$, and Temporal Adapter $P_{TE} \in \mathbb{R}^{L \times C}$ as $P_d = P_{TO}^d + P_{PO}^d + P_{TE}^d$, where $d \in \{\text{Trend, Seasonal, Residual}\}$, this means that we can obtain P_{Trend} , $P_{Seasonal}$, $P_{Residual}$.

B.6 Theoretical Insights on Personalized Adapter

The effectiveness and superiority of our proposed Personalized Adapter have been demonstrated in sufficient ablation studies (please refer to **Table 6** in the main text). Here, we will discuss theoretical insights that further supports the effectiveness of Personalized Adapter. Personalized Adapter can effectively capture potential pattern in meteorological variable time series, which comprises both the Task Adapter and the FFN-based Parameter Adapter. Specifically, our focus primarily revolves around the Task Adapter active in extracting representations, which including Token/Positional/Temporal Embedding for transforming meteorological variable time series.

Let the weather sequence be $\mathbf{X} = (\mathbf{x}_1, \mathbf{x}_2, \dots, \mathbf{x}_T)$, where $\mathbf{x}_t \in \mathbb{R}^d$ is the observed value with d variables at t moment. Let \mathcal{X} represent the function space to which \mathbf{x}_t of a weather sequence belongs, and \mathcal{Z} denote the function space to which the implicit representation \mathbf{z}_t belongs. Token Embedding can be interpreted as a mapping $f_{\theta} : \mathcal{X} \rightarrow \mathcal{Z}$. According to the Kolmogorov-Arnold representation theorem, for any continuous function $f \in C([0, 1]^d)$, there exist $2d + 1$ continuous functions $\phi_q \in C([0, 1])$ and $\psi_q \in C([0, 1])$ such:

$$f(\mathbf{x}) = \sum_{q=0}^{2d} \phi_q \left(\sum_{p=1}^d \psi_q(x_p) \right),$$

which means Token Embedding can construct a high-dimensional nonlinear mapping from multiple one-dimensional functions, capturing complex patterns within weather sequences. Positional Embedding introduces a vector \mathbf{p}_t for each step, enabling the model to differentiate between observations at different time steps. For any two steps t_1 and t_2 , their position vectors \mathbf{p}_{t_1} and \mathbf{p}_{t_2} satisfy:

$$\|\mathbf{p}_{t_1} - \mathbf{p}_{t_2}\|_2 = \sqrt{2k(1 - \cos \frac{2\pi(t_1 - t_2)}{10000^{1/k}})}.$$

The growing distance between t_1 and t_2 with an increasing time gap mirrors the relative positioning of time steps, aiding the model in grasping temporal dependencies. Additionally, the sine-cosine function’s periodicity resonates with weather data’s cyclical behavior, helping the model to learn from these recurrent patterns.

Finally, consider the role of Temporal Embedding from the view of matrix decomposition. Suppose the temporal matrix \mathbf{T} has a rank of r , it can be decomposed as $\mathbf{z}_t \otimes \mathbf{T} = \sum_{i=1}^r (\mathbf{z}_t \otimes \mathbf{u}_i) \mathbf{v}_i^T$. Temporal Embedding transforms the original sequence by scaling and rotating it to represent different interaction patterns. Using singular value decomposition, the top r singular vectors distill the core structure of the time-based matrix. This allows Temporal Embedding to intuitively learn a compact representation of weather sequences, highlighting the primary interactions between variables. In optimizing Personalized Adapter within LM-WEATHER, the focus lies solely on Personalized Adapter and the attention layer influenced by LoRA during local updates. As Personalized Adapter undergoes solely local updates while sharing low-rank matrices globally, akin to layer-wise optimization in PLM, the efficacy of its optimization process can be theoretically substantiated by the theoretical analysis provided in [47].

B.7 Evaluation Metrics

For evaluation metrics, as [48], we utilize the mean absolute error (MAE) and root mean square error (RMSE) for both forecasting and imputation. The calculation of these metrics are as follows:

$$\text{MAE} = \frac{1}{T} \sum_{i=1}^T |\mathbf{Y}_i - \hat{\mathbf{Y}}_i|, \quad \text{RMSE} = \sqrt{\frac{1}{T} \sum_{i=1}^T (\mathbf{Y}_i - \hat{\mathbf{Y}}_i)^2}, \quad (11)$$

where T denotes the number of data points (*i.e.*, prediction horizon in our cases), \mathbf{Y}_i and $\hat{\mathbf{Y}}_i$ are the i -th ground truth and prediction where $i \in \{1, \dots, T\}$.

B.8 Model Configurations

The configurations of our LM-WEATHER for different tasks and datasets are summarized in **Tab. 15**. We consistently use the AdamW [49] optimizer in all experiments.

Table 15: An overview of the experimental configuration for LM-WEATHER. LR is the initial learning rate, (FS) denotes the few-shot learning setting.

Task-Dataset / Configuration	Model Hyperparameter				Training Process					
	Backbone (PLM) Layers	Input Length	Patch Dim	Heads	LR	Loss	Batch Size	Local Epochs	Communication Round	participation rate
Forecasting - ODW1T	5	192	16	8	0.005	MSE	128	20	50	0.1
Forecasting - ODW1V	5	192	16	8	0.005	MSE	128	20	50	0.1
Forecasting - ODW2T	5	192	16	8	0.005	MSE	256	20	50	0.1
Forecasting - ODW2V	5	192	16	8	0.005	MSE	256	20	50	0.1
Imputation - ODW1T	5	96, 192, 336, 720	16	8	0.005	MSE	128	20	50	0.1
Imputation - ODW1V	5	96, 192, 336, 720	16	8	0.005	MSE	128	20	50	0.1
Imputation - ODW2T	5	96, 192, 336, 720	16	8	0.005	MSE	256	20	50	0.1
Imputation - ODW2V	5	96, 192, 336, 720	16	8	0.005	MSE	256	20	50	0.1
Forecasting - ODW1T (FS)	5	192	16	8	0.005	MSE	128	20	50	0.1
Forecasting - ODW1V (FS)	5	192	16	8	0.005	MSE	128	20	50	0.1
Forecasting - ODW2T (FS)	5	192	16	8	0.005	MSE	256	20	50	0.1
Forecasting - ODW2V (FS)	5	192	16	8	0.005	MSE	48	20	50	0.1
Imputation - ODW1T (FS)	5	96, 192, 336, 720	16	8	0.005	MSE	128	20	50	0.1
Imputation - ODW1V (FS)	5	96, 192, 336, 720	16	8	0.005	MSE	128	20	50	0.1
Imputation - ODW2T (FS)	5	96, 192, 336, 720	16	8	0.005	MSE	256	20	50	0.1
Imputation - ODW2V (FS)	5	96, 192, 336, 720	16	8	0.005	MSE	48	20	50	0.1

Appendix C Theorems and Proofs

Theorem C.1 (Decomposition Rationality from Time Series). *Given a weather time series $\mathcal{X} = \mathcal{X}_{\text{Trend},t} + \mathcal{X}_{\text{Seasonal},t} + \mathcal{X}_{\text{Residual},t}$, $t \in [t_1, t_n]$. Let $\mathbf{E} = \{e_1, e_2, \dots, e_n\}$ denotes a set of orthogonal bases. Let $\mathbf{E}_{\text{Seasonal}} \subseteq \mathbf{E}$ denote the subset of \mathbf{E} on which $\mathcal{X}_{\text{Seasonal},t}$ has non-zero eigenvalues and $\mathbf{E}_{\text{Trend}} \subseteq \mathbf{E}$ denote the subset of \mathbf{E} on which $\mathcal{X}_{\text{Trend},t}$ has non-zero eigenvalues. If $\mathcal{X}_{\text{Trend},t}$ and $\mathcal{X}_{\text{Seasonal},t}$ are not orthogonal, *i.e.*, $\sum_{i=1}^n \mathcal{X}_{\text{Trend},t}^i \mathcal{X}_{\text{Seasonal},t}^i \neq 0$, then $\mathbf{E}_{\text{Trend}} \cap \mathbf{E}_{\text{Seasonal}} \neq \emptyset$, *i.e.*, \mathbf{E} can not disentangle the two signals onto two disjoint set of bases.*

Proof. We decompose $\mathcal{X}_{\text{Seasonal},t}$ and $\mathcal{X}_{\text{Trend},t}$ onto \mathbf{E} and acquire that $\mathcal{X}_{\text{Seasonal},t} = \sum a_i e_i$ and $\mathcal{X}_{\text{Trend},t} = \sum b_i e_i$. Then it is obvious that $e_i \in \mathcal{X}_{\text{Seasonal}} \Leftrightarrow a_i \neq 0$ and $e_i \in \mathcal{X}_{\text{Trend}} \Leftrightarrow b_i \neq 0$. Now, let us consider the

inner product of $\mathcal{X}_{\text{Seasonal},t}$ and $\mathcal{X}_{\text{Trend},t}$:

$$\begin{aligned} \sum_{i=1}^n \mathcal{X}_{\text{Trend},t}^i \mathcal{X}_{\text{Seasonal},t}^i &= \mathcal{X}_{\text{Trend},t} \mathcal{X}_{\text{Seasonal},t} \\ &= \left(\sum a_i e_i \right) \cdot \left(\sum b_i e_i \right) = \sum_{i,j} a_i b_j e_i e_j \end{aligned} \quad (12)$$

Note that $\sum_{i=1}^n \mathcal{X}_{\text{Trend},t}^i \mathcal{X}_{\text{Seasonal},t}^i = 0$. Thus, there must be at least one i such that $a_i \neq 0$ and $b_i \neq 0$. Thus, $e_i \in \mathbf{E}_{\text{Seasonal}}$ and $e_i \in \mathbf{E}_{\text{Trend}}$, in other words, $\mathbf{E}_{\text{Trend}} \cap \mathbf{E}_{\text{Seasonal}} \neq \emptyset$. The theorem demonstrates that if $\mathcal{X}_{\text{Trend},t}$ and $\mathcal{X}_{\text{Seasonal},t}$ are not orthogonal, orthogonal bases that separate $\mathcal{X}_{\text{Trend},t}$ and $\mathcal{X}_{\text{Seasonal},t}$ into two distinct sets cannot exist. Typically, periodic and non-periodic signals are not orthogonal because the periodic signal has a discrete spectrum, while the non-periodic signal has a continuous one, leading to potential overlaps at non-zero frequencies. Principal Component Analysis (PCA) seeks to find orthogonal bases in data, but it cannot split these two signals into separate bases. Citing Theorem 1 from [17], we understand that self-attentive mechanisms in pre-trained large models function similarly to PCA. Thus, without manual intervention, the self-attentive mechanism is unable to automatically divide a time series into trend and seasonal components. \square

Theorem C.2 (Exchange Low-Rank Matrices Ensures Privacy). *Given a on-device weather modeling framework based on federated learning that gloabl optimization object is $\mathbf{F}(\theta) = \sum_{i=1}^n p_i f(\{D_i\}; \theta)$, where $f(x; \theta)$ is the loss function of i -th client, $\{D_i\}$ is dataset of i -th client, and p_i and θ denote the data distribution weight of client i and the model parameters, respectively. Given that the parameters θ of the PLM \mathcal{M}_θ broadcasted by the server consist of two parts: a frozen part $\mathcal{M}_{\theta,f}$ and a trainable part $\mathcal{M}_{\theta,t}$, interacting only the low-rank matrix parameters $\mathcal{M}_{\theta,l} \subset \mathcal{M}_{\theta,t}$ is a subset of trainable part $\mathcal{M}_{\theta,t}$ during each round ensures privacy.*

Proof. We assume that $f(x; \theta)$ is a convex function with respect to θ , i.e., for any θ_1 and θ_2 and $\lambda \in [0, 1]$, we have

$$f(x; \lambda\theta_1 + (1 - \lambda)\theta_2) \leq \lambda f(x; \theta_1) + (1 - \lambda)f(x; \theta_2). \quad (13)$$

Since only low-rank matrices parameter $\mathcal{M}_{\theta,l}$ parameterized by θ_l is exchanged, we can convert θ to $\theta' = [\theta'_l, \theta_o]$, where θ'_l is the embedding parameter after the server update. Since we only update on θ_l , θ_o remains unchanged. Thus, data privacy can be ensured, as θ_o contains parameters that reveal user-specific information. Furthermore, the low-rank matrices applied to the PLM \mathcal{M}_θ using LoRA are initialized with a random Gaussian distribution and all-zero values, respectively, before training. This global information sharing approach also helps to enhance privacy. \square

Appendix D Additional Finding & Experiment & Discussion

In this section, we explore and discuss potential research findings and questions for our LM-WEATHER via conducting additional experiments. These potential research questions are as follows:

- **RQ1.** How does LM-WEATHER compare to Personalized Federated Learning (PFL) baselines in terms of trade-offs in personalization and global model performance?
- **RQ2.** How does LM-WEATHER compare to other FL baselines focused on improving communication efficiency?
- **RQ3.** How does LM-WEATHER perform compared to centralized and local-only training modes?
- **RQ4.** How does the pre-trained language model contribute in LM-WEATHER?
- **RQ5.** How robust in LM-WEATHER to the number of participating training devices?
- **RQ6.** What is the resource utilization and training & inference cost of LM-WEATHER?
- **RQ7.** Can LM-WEATHER be used for other tasks?

D.1 Trade-offs in Personalization and Global Model Performance (RQ1)

Our LM-WEATHER builds on the assumption that the foundation model already exists, treating pre-trained language models (PLMs) as such and broadcasting it to each client to achieve local updates. Our aim is to employ device information-specific (e.g., geographic/atmospheric patterns) adapter, to promote the local PLM in achieving cross-domain knowledge transfer from language to meteorological sequences. This approach yields highly customized models for individual devices while achieving global knowledge to avoid data silo, thereby supporting diverse analyses of heterogeneous weather data. Alternative PFL methods do not match the efficiency and flexibility of our personalized adapter in this context, making them less suitable. By incorporating PFL baselines (Per-FedAvg [38], APPLE [50], FedPer [51], and FedALA [52]), we provide quantitative results that substantiate our claims, experiment setting is consistent with the manuscript on ODWIT.

PFL Baseline. A brief description of PFL baselines used in this section of the experiment is as follows.

- **Per-FedAvg:** Allowing for personalized model updates for each client by adding client-specific parameters to the global model and optimizing them during FL training.
- **APPLE:** Tackling statistical heterogeneity in FL by automatically capturing information required by clients from global models using adaptive local aggregation methods.
- **FedPer:** Dividing the model into a base layer and a personalization layer, only the base layer is uploaded during aggregation while keeping the personalization layer to combat statistical heterogeneity.
- **FedALA:** Tackling statistical heterogeneity in FL by automatically capturing information required by clients from global models using adaptive local aggregation methods.

Table 16: Comparison on personalized performance between our LM-WEATHER and PFL baselines under forecasting (multivariate-multivariate) and imputation (50% masking rate), where Avg. denotes the average performance of four periods [96, 192, 336, 720], **Bold** means the best.

Task / Method	LM-WEATHER (Ours)	Per-FedAvg	APPLE	FedALA	FedPer
Forecasting (Avg.)	45.4/74.6	48.6/76.7	51.7/79.0	50.4/80.0	52.1/79.0
Imputation (Avg.)	23.1/42.4	27.7/50.1	26.5/49.6	34.4/57.2	30.2/54.0
Forecasting (Avg., 5% Few-Shot)	89.7/96.7	101.4/197.3	99.6/186.2	117.3/214.0	104.9/202.8
Imputation (Avg., 5% Few-Shot)	62.3/124.4	89.2/177.8	92.1/199.2	82.4/153.7	84.9/159.7

Personalized Performance Comparison. The performance quantification of our LM-WEATHER and PFL baselines under personalized performance for different tasks and scenarios is shown in Table 16. Our LM-WEATHER outperform other PFL baselines across different tasks (forecasting/imputation) and scenarios (regular/few-shot learning) by a wide margin. This supports our finding that in the scenario of on-device weather variable modeling, PFL methods is not appropriate.

Global Model Performance Comparison. The comparison on global model performance across client between our LM-WEATHER and PFL baselines are shown in Table 16. Our LM-WEATHER outperforms PFL baselines in terms of global model performance, as demonstrated by the fact that its global model performs more stable across client with heterogeneous data.

Table 17: Comparison on global model performance across client between LM-Weather and PFL baselines on multivariate-multivariate forecasting tasks (OWD1T dataset, MAE/RMSE report), **Red** denotes the original LM-WEATHER’s performance, and **Bold** means the best among global performance.

Client ID	LM-WEATHER (Ours)	LM-WEATHER (Global)	Per-FedAvg (Global)	APPLE (Global)	FedALA (Global)	FedPer (Global)
1	44.8/73.9	42.5/69.4	50.3/78.2	53.4/77.1	51.7/76.3	52.8/82.5
2	46.1/75.4	56.8/84.7	61.8/90.1	64.7/88.6	63.2/88.1	68.3/99.8
3	45.2/74.3	49.3/75.2	54.2/82.6	57.2/81.4	55.9/80.7	57.1/87.2
4	47.1/79.0	61.2/89.6	64.9/93.4	67.8/92.1	66.5/91.6	73.6/105.3
5	43.1/70.6	45.7/72.1	52.1/80.3	55.1/78.9	53.6/78.2	54.9/84.6
6	43.3/73.7	59.1/87.3	63.4/91.7	66.3/90.3	64.8/89.5	70.2/102.1
7	44.8/74.1	47.6/73.8	55.9/84.5	58.9/83.2	57.3/82.4	59.5/89.9
8	48.1/77.2	53.4/80.5	59.6/88.5	62.6/87.4	61.1/86.6	65.7/96.4
9	42.6/71.7	44.1/70.7	50.9/78.8	53.8/77.6	52.3/76.9	53.6/83.3
10	46.0/75.3	57.9/86.2	64.2/92.6	67.1/91.5	65.7/90.6	71.9/103.7
11	45.3/74.4	50.2/76.3	54.7/83.2	58.0/82.3	56.6/81.3	60.8/91.6
12	45.6/74.9	55.7/82.9	60.8/89.4	63.9/88.5	62.5/87.7	67.4/98.2
13	48.7/77.8	43.3/68.5	49.6/77.5	56.3/76.3	50.9/75.5	51.7/81.1
14	49.2/75.5	60.5/88.4	65.7/94.2	68.7/92.8	67.4/92.4	72.5/104.5
15	41.1/73.2	48.7/74.4	53.4/81.9	56.3/80.2	54.5/79.4	58.2/88.5
Total (Avg.)	45.4/74.6	51.2/78.7	57.0/84.9	59.9/83.2	58.4/82.8	61.4/92.7

Personalization and Global Model Performance Trade-offs. We consider the trade-off between personalization performance and global model performance for our LM-WEATHER and PFL baselines, the results are shown in Table 18. Compared with PFL baselines, our LM-WEATHER maintains the best trade-off between personalization performance and global model performance, *i.e.*, the personalization performance does not significantly exceed the global model performance while the performance far exceeds PFL methods, which means that the LM-WEATHER can be flexibly applied to different practical scenarios, including personalised analysis of regional weather trends as well as comprehensive analysis of weather trends over large-scale regions. This means that LM-WEATHER can be flexibly applied to different practice scenarios, including the personalised analysis of regional weather trends and the comprehensive analysis of weather trends over large scale areas.

Table 18: Comparison of LM-Weather between personalized performance and global model performance, results are obtained on the multivariate-multivariate forecasting task on OWD1T (MAE/RMSE report), **Bold** means the best, \uparrow represents the improvement (gap) in the personalization performance of the method relative to the global model performance.

Method	Personalized Performance	Global Model Performance	Ave. Variation (Personalized vs. Global)
Per-FedAvg	48.6/76.7	57.0/84.9	\uparrow 13.99%
APPLE	51.7/79.0	59.9/83.2	\uparrow 10.58%
FedALA	50.4/80.0	58.4/82.8	\uparrow 9.68%
FedPer	52.1/79.0	61.4/92.7	\uparrow 17.59%
LM-WEATHER (Ours)	45.4/74.6	51.2/78.7	\uparrow 9.16%

Performance and Adapter Updating Trade-offs. Furthermore, we investigated the effect of varying the number of local update rounds in adapters across clients on the performance of LM-WEATHER regarding personalization. The results are presented in **Table 19**. We observed that increasing the local update rounds from the default five to fifteen leads to smoother and enhanced personalization performance across heterogeneous clients. However, this increase in local update rounds also incurs additional computational and communication costs, which, in our assessment, do not justify the modest performance improvements.

Table 19: Performance of each client under the multivariate-multivariate forecasting task on ODWT1 with different adapter local update epoch (MAE/RMSE report), where $E = 5/10/15$ represent the 5, 10, and 15 local training rounds, respectively.

Client ID	LM-WEATHER ($E = 5$)	LM-WEATHER ($E = 10$)	LM-WEATHER ($E = 15$)
1	44.8/73.9	41.3/70.5	41.6/69.7
2	46.1/75.4	47.9/75.8	46.3/74.5
3	45.2/74.3	43.5/72.1	43.1/71.1
4	47.1/79.0	46.2/74.6	45.7/73.6
5	43.1/70.6	42.7/71.3	42.4/70.4
6	43.3/73.7	45.5/74.2	44.9/73.0
7	44.8/74.1	44.1/73.0	43.5/71.7
8	48.1/77.2	48.6/76.3	47.2/75.2
9	42.6/71.7	40.9/70.1	41.2/69.3
10	46.0/75.3	46.8/75.4	45.3/74.1
11	45.3/74.4	43.2/71.8	42.8/70.8
12	45.6/74.9	45.7/74.5	44.5/72.7
13	48.7/77.8	42.1/70.9	41.9/70.1
14	49.2/75.5	47.3/75.1	46.8/74.9
15	41.1/73.2	44.8/73.4	43.8/72.3
Total (Avg.)	45.4/74.6	44.6/73.2	44.0/72.2

D.2 Communication Efficiency (RQ2)

We have shown the communication efficiency of our LM-WEATHER in **Table 7**, all baseline achieve a 100% rank as they exchange all local parameters during communication. However, we acknowledge that solely comparing the communication parameter ratio doesn't provide a holistic view of LM-WEATHER's communication effectiveness, as some baselines inherently possess fewer parameters. To address this and further validate the excellent communication efficiency of our LM-WEATHER, we introduce quantitative comparisons by including FL methods tailored to improve communication efficiency (FedKD [53], FedPAQ [54], FedBF [55], FedAP [55], PromptFL [56]) as baselines.

Baseline. A brief description of these FL methods tailored to improve communication efficiency is as follows.

- **FedKD:** This parameter-efficient PFL method integrates knowledge distillation within a single client and employs a parameter aggregation strategy using Singular Value Decomposition (SVD). For the purposes of this section, which focuses solely on comparing communication efficiency, we incorporate only the SVD-based client-server communication strategies into LM-WEATHER as a baseline.

- **FedPer**: This PFL approach maintains a personalized layer while sharing the remaining base layers during communication. This enhances communication efficiency by transmitting only a portion of the parameters.
- **FedBF**: This fine-tuning method enhances parameter efficiency by sharing only the biases of the local model during global aggregation, thereby reducing communication overhead. To integrate this method into LM-WEATHER as a baseline, we adjusted all biases in LM-WEATHER to be unfrozen.
- **FedAP**: A parameter-efficient fine-tuning method in FL, which involves sharing only adapters during global aggregation.
- **PromptFL**: This parameter-efficient FL method enables participants to cooperatively train lightweight prompts without sharing the entire model, significantly accelerating both local training and global aggregation. In our experiments, we treat the adapter generated on clients as the prompt to facilitate the incorporation of this baseline.

Quantitation Results and Comparison. The results is shown in **Table 20**, compared to LM-WEATHER-Ave (serve as the standard line), our LM-WEATHER achieves a significant improvement in communication efficiency while maintaining excellent performance. Additionally, LM-WEATHER significantly outperforms baseline in terms of both communication efficiency and performance across different tasks. Even when compared to lightweight baselines (i.e., FL-LightTS/DLinear), LM-WEATHER continues to outperform them. This underscores LM-WEATHER’s superiority in both communication efficiency and performance.

Table 20: Comparison of LM-WEATHER and baseline that tailored to improve communication efficiency in terms of forecasting (multivariate-multivariate)/imputation (50% masking rate) performance as well as communication efficiency, with \times denotes the improvement in communication efficiency relative to the standard line (LM-WEATHER-Ave), MAE/RMSE report, and **Bold** means the best.

Method	Forecasting	Imputation	Train.	Comm. Params.	Comm.
FL-Pyraformer	73.0/91.3	68.0/89.7	153.32 M	153.32 M	0.07 \times
FL-PatchTST	48.6/81.0	45.4/73.5	74.74 M	74.74 M	0.14 \times
FL-LightTS	62.7/93.4	26.1/45.7	1.68 M	1.68 M	6.2 \times
FL-DLinear	63.3/82.8	28.5/49.9	1.06 M	1.06 M	9.8 \times
LM-WEATHER-Ave	47.5/78.7	24.0/44.1	10.38 M	10.38 M	1 \times
LM-WEATHER (Ours)	45.4/74.6	23.1/42.4	10.38 M	0.38 M	27.3\times
LM-WEATHER (w FedKD)	49.6/76.2	27.5/43.6	10.38 M	1.68 M	6.2 \times
LM-WEATHER (w FedPer)	52.1/79.0	25.1/44.3	10.38 M	8.46 M	1.2 \times
LM-WEATHER (w FedBF)	46.2/78.1	23.7/44.0	10.49 M	10.49 M	0.9 \times
LM-WEATHER (w FedAP)	47.4/79.2	24.3/44.7	10.38 M	9.6 M	1.1 \times
LM-WEATHER (w PromptFL)	46.0/78.4	23.8/45.1	10.38 M	8.4 M	1.2 \times

D.3 Centralised and Local-only Training (RQ3)

The ordinary centralised training strategy (all data were aggregated into a single server) exhibits learning efficiency that an ordinary distributed learning strategy. The ultimate goal of FL is to achieve performance close to that of centralised training and to ensure privacy across data sources. **Table 21** illustrates that our LM-WEATHER achieves comparable effectiveness to Non-FL (centralised) training, with only a 2.04% disparity. Compared to LM-WEATHER-Local, which lacks interaction between devices, LM-WEATHER performs better due to overcoming data silos.

D.4 Contributions of Pre-trained Language Model in LM-WEATHER (RQ4)

Our LM-WEATHER significantly outperforms time series-specific models trained from scratch under centralised setup. Centralised training aims to acquire an excellent pre-trained model, where PLMs possess inherent advantages due to their prior sequence modeling capabilities. Moreover, various parameter-efficient fine-tuning (PEFT) strategies enable PLMs to adapt to new domain knowledge cost-effectively. FL-based aggregation facilitates a stable on-device fine-tuning process, with LM-Weather enabling highly customized on-device fine-tuning of PLMs with greater efficiency. This highlights the substantial contribution of PLMs in this task.

D.5 Robustness to Number of Devices (RQ5)

During our main experiments, we maintained a device participation rate of 0.1, meaning that 2 devices (for ODW1) and 4 devices (for ODW2) were randomly selected for updating in each communication round. We

Table 21: Comparison of LM-WEATHER’s multivariate-multivariate performance in the FL and the Non-FL (centralised) setups, LM-WEATHER-Local is the setting in which LM-WEATHER is trained locally at each device without communication, and disparity is the difference in performance relative to Non-FL.

Dataset	Length	Non-FL (centralised)	LM-WEATHER (Ours)	LM-WEATHER-Ave	LM-WEATHER-Local
ODW1T	96	41.7/70.3	42.3/71.1	44.1/74.8	45.9/72.9
	192	43.5/71.6	44.4/73.6	46.3/77.5	46.7/74.3
	336	45.2/72.9	45.8/75.2	47.9/79.3	48.2/77.0
	720	46.8/73.6	49.2/78.5	51.8/83.0	50.5/80.5
	Avg.	44.3/72.1	45.4/74.6	47.5/78.7	47.8/76.2
ODW1V	96	42.3/68.7	42.3/69.6	42.7/69.5	44.5/68.6
	192	43.9/69.9	44.4/71.7	45.5/72.6	46.1/70.4
	336	45.4/71.2	46.0/72.4	47.2/74.3	48.8/73.2
	720	46.8/72.6	49.7/74.0	51.2/78.2	53.2/79.4
	Avg.	44.6/70.6	45.6/71.9	46.6/73.6	48.2/72.9
Communication Param. #		None	0.38 M	10.38 M	Not applicable
Disparity		0	↓ 2.04%	↓ 4.37%	↓ 5.67%

Table 22: Comparison between fine-tuning PLM with Adapter (LM-WEATHER) and training from scratch using non-PLM architecture (Pyraformer, Reformer, PatchTST, DLinear, and LightTS) on multivariate-multivariate forecasting tasks (MAE/RMSE report), **Bold** means the best.

Dataset	Length	LM-WEATHER (Ours)	Pyraformer	Reformer	PatchTST	Dlinear	LightTS
ODW1T	96	43.0/75.2	66.0/84.2	68.2/89.6	44.7/76.1	48.6/77.6	52.1/83.3
	192	44.7/78.4	68.7/87.4	69.3/89.9	46.5/78.4	51.0/79.8	57.5/87.0
	336	47.2/80.9	71.3/90.9	71.4/91.7	48.2/80.3	52.3/84.1	62.3/94.2
	720	50.4/83.8	76.8/92.3	74.5/93.9	54.2/84.5	55.4/86.3	69.5/98.4
	Avg.	46.3/79.6	70.7/88.7	70.9/91.3	48.4/79.8	51.8/82.0	60.4/90.7
ODW1V	96	45.4/71.3	60.4/69.1	45.7/71.8	47.2/73.4	48.5/74.7	50.1/75.3
	192	46.9/72.9	61.9/73.2	51.9/75.5	48.4/74.2	49.4/76.6	52.7/78.8
	336	49.0/75.5	64.4/76.9	53.4/76.9	48.9/76.7	53.7/78.3	54.0/80.4
	720	53.7/79.1	68.2/82.7	56.5/84.9	54.1/77.4	57.2/82.2	57.7/84.8
	Avg.	48.8/74.9	63.7/75.5	51.9/77.3	49.7/75.4	52.2/78.0	53.6/79.8
1 st Count		16	1	0	3	0	0

incorporated quantitative analysis results on ODW1T and ODW1V dataset showcasing the impact of varying the number of devices across different tasks (Table 23). Additionally, we provided the percentage change in performance relative to the default number of devices to assess LM-WEATHER’s robustness to device count fluctuations. Our analysis reveals that LM-Weather exhibits robustness to changes in the number of devices, stemming from several factors: (1) Increasing the number of devices during training, both in regular and few-shot scenarios, marginally improves LM-Weather’s performance in most cases, with fluctuations confined within a stable range. (2) Performance gains from additional devices are not strictly proportional, as introducing more devices can also lead to decreased performance due to data distribution imbalances, resulting in overall performance impairment. (3) The addition of more devices entails greater communication burdens, which may not be cost-effective for minor performance gains, particularly in resource-constrained environments. These findings underscore LM-WEATHER’s relative resilience to device count variations and its ability to strike an optimal balance between performance enhancement and communication overhead.

D.6 No Free Lunch in Performance Improvement (RQ6)

The remarkable capabilities of cutting-edge DL models across various domains and tasks, such as LLMs, and VLMs, can be attributed to their extensive parameters and training on large datasets. Currently, a perfect balance among performance, model size, and cost does not exist. Despite numerous studies focusing on reducing training and inference costs while maintaining superior performance, there is no one-size-fits-all solution. This is also true for our LM-WEATHER, which demonstrates exceptional performance across diverse tasks and scales on real-world datasets with significant heterogeneity, significantly outperforming comparable DL methods. In this context, we analyze the costs associated with training and inference for LM-WEATHER and its baselines, exploring and discussing the trade-offs between cost-effectiveness and performance in practical applications.

The quantification and comparison of computational costs against LM-WEATHER and baseline are shown in Table 24. We discuss this results from two perspectives as follow.

Table 23: Results of LM-WEATHER under Forecasting (multivariate-multivariate) and Imputation (50% masking rate) at different device participation rates [0.1, 0.3, 0.5, 0.7, 0.9], \uparrow/\downarrow implies an increase/decrease in performance relative to the original setting (0.1), MAE/RMSE report, where 15% represents the proportion of data on each client involved in training.

Dataset	Rate / Devices	Normal		Few-Shot (15%)	
		Forecasting	Imputation (50 % masked)	Forecasting	Imputation (50 % masked)
ODW1T	0.1 (2/round)	44.4/73.6	22.6/42.0	64.7/100.4	40.2/68.2
	0.3 (5/round)	43.7/72.5 (\uparrow 1.55)	24.2/43.7 (\downarrow 5.55)	63.4/99.7 (\uparrow 1.40)	41.4/68.7 (-1.85)
	0.5 (8/round)	42.9/72.0 (\uparrow 2.85)	21.0/42.1 (\uparrow 3.90)	63.7/99.2 (\uparrow 1.40)	42.3/68.5 (\downarrow 2.8)
	0.7 (11/round)	43.9/74.1 (\uparrow 0.25)	21.8/41.2 (\uparrow 2.80)	64.5/101.0 (\uparrow 0.10)	39.5/66.7 (\uparrow 2.00)
	1.0 (16/round)	44.2/74.0 (0 -)	21.3/41.6 (\uparrow 3.10)	63.6/100.2 (\uparrow 0.95)	40.4/68.0 (\downarrow 0.1)
ODW2T	0.1 (4/round)	66.2/89.1	37.2/54.9	89.7/131.8	77.2/112.6
	0.3 (11/round)	68.2/89.7 (\downarrow 1.85)	36.5/53.1 (\uparrow 2.65)	90.2/132.5 (\downarrow 0.55)	75.4/110.3 (\uparrow 2.25)
	0.5 (18/round)	65.4/89.2 (\uparrow 0.55)	36.7/53.4 (\uparrow 2.05)	89.1/131.4 (\uparrow 0.50)	76.5/111.2 (\uparrow 1.10)
	0.7 (25/round)	65.7/88.8 (\uparrow 0.90)	36.1/53.9 (\uparrow 2.45)	88.9/130.9 (\uparrow 0.80)	76.9/112.3 (\uparrow 0.35)
	1.0 (36/round)	65.9/89.0 (\uparrow 0.25)	36.9/55.0 (\uparrow 0.30)	89.1/130.7 (\uparrow 0.75)	76.7/112.1 (\uparrow 0.50)

Table 24: Comparison of training/inference costs based on ODW1T with $N = 192$ under multivariate-multivariate forecasting tasks (MAE/RMSE report), where **Bold** denotes the best, ‘Comm.’ and ‘Perf.’ denote communication and performance, respectively.

Method	Ave. Training Time (per round)	Inference Time (per client)	Training Memory (per client)	Inference Memory (per client)	Comm. Time	Perf.
FL-DLinear	4 s	1 s	7.93 MB	4.21 MB	1.44 s	52.3/81.8
FL-LightTS	4 s	2 s	30.94 MB	17.24 MB	9.93 s	59.5/90.6
FL-PatchTST	124 s	10 s	1260.01 MB	660.02 MB	59.62 s	47.3/79.8
FL-Transformer	121 s	11.0 s	1700.95MB	841.09 MB	36.44 s	52.1/84.0
FL-iTransformer	9 s	1.6 s	705.36 MB	372.28 MB	22.40 s	51.8/84.3
FL-Informer	110 s	10 s	1890.00 MB	897.21 MB	42.81 s	52.9/84.6
FL-Reformer	145 s	17.7 s	786.98 MB	421.23 MB	16.72 s	75.1/98.3
FL-Pyraformer	80 s	8.1 s	1880.41 MB	950.77 MB	119.66 s	70.0/90.9
FL-GPT4TS	108 s	21.2 s	3640.11 MB	1900.98 MB	10.03 s	48.6/81.3
LM-WEATHER	91 s	14 s	3014.82 MB	1500.81 MB	0.29 s	44.4/73.6

Communication and Performance. LM-WEATHER outperforms baseline in these two key metrics, which is critical for practical meteorological variable modeling and analysis, a bandwidth-sensitive and high accuracy demanding application.

Trade-offs between Resource Consumption and Performance. In terms of training and inference time and memory usage, LM-WEATHER is less efficient than lightweight baselines such as FL-DLinear, LightTS, and iTransformer, due to its use of a Pretrained Language Model (PLM) as a backbone. Although LM-WEATHER demands more resources, the trade-off is justified by its cost-effective performance gains. Its slightly increased memory requirements for training and inference are manageable on most devices. In the context of weather analysis, where precision is critical, prioritizing performance improvements over minimal resource consumption is essential. Additionally, LM-WEATHER capitalizes on the knowledge-rich PLM and requires only minimal, low-cost fine-tuning on devices to achieve superior performance. This strategy not only enhances performance but also reduces the frequency of future model updates, thereby lowering long-term costs compared to developing a baseline model from scratch.

Table 25: Comparison between LM-Weather and baseline in terms of model size on the device and performance of forecasting (multivariate-to-multivariate), and imputation (50% masking rate) on ODW1T (MAE/RMSE report), where **Bold** and Underline denote the best and the second best.

Method	Size	Forecasting	Imputation
FL-DLinear	0.28 M	53.3/82.8	28.5/49.9
FL-LightTS	<u>1.10 M</u>	62.7/93.4	26.1/45.7
FL-PatchTST	37.61 M	48.6/81.0	45.4/73.5
FL-Transformer	45.55 M	52.8/84.7	57.6/82.3
FL-iTransformer	25.19 M	53.7/63.7	27.6/48.2
FL-Informer	52.31 M	53.4/85.2	61.4/85.9
FL-Reformer	45.59 M	78.2/98.7	69.8/92.5
FL-GPT4TS	321.7 M	<u>49.9/82.5</u>	<u>25.1/46.2</u>
LM-WEATHER	304.1 M	45.4/74.6	23.1/42.4

In addition, we further provide a comparison of model sizes and performance between LM-WEATHER and baseline, as shown in **Table 25**. The difference in model size between our LM-WEATHER and baseline can be deemed acceptable for the following reasons.

Trade-offs between Performance and Size. While LM-WEATHER may not be as compact in terms of model size or resource efficiency as lightweight baselines, it offers significant advantages in various analysis tasks. Its high performance is particularly valuable in practical applications. Moreover, with a model size of 304.19 M, LM-WEATHER is still accessible for devices with limited resources. This contrasts sharply with many large foundation models, which typically comprise several hundred million parameters. The trade-off between performance and size is justified, especially considering the critical nature of accurate weather data analysis.

Efficient Parameter Update and Communication. LM-WEATHER implements efficient on-device fine-tuning of the pretrained language model. Unlike baselines that require training from scratch, LM-WEATHER only needs fine-tuning of a relatively small number of parameters (10.38 M) on each device, with minimal device-to-server communication overhead (0.38 M). This approach facilitates highly personalized cross-domain knowledge transfer, significantly reducing the ongoing costs associated with processing the ever-changing streams of weather data. These aspects highlight the pragmatic considerations that have shaped the design of LM-WEATHER. The model’s capabilities to deliver exceptional performance, combined with its efficient parameter tuning and communication strategies, offer a cost-effective solution for advanced weather data analysis in resource-constrained environments.

D.7 Additional Tasks for Potential Applications (RQ7)

Given datasets we proposed in this paper focus on forecasting and imputation tasks, we broaden its scope briefly to explore its potential application by integrating anomaly weather detection tasks. This involves relabeling the dataset to identify intervals with anomalous meteorological variables as instances of abnormal weather processes. Specifically, we label original datasets via Isolation Forest [57], the main process as follows: (1) We set the cut length to 100, using this metric to segment each channel (variable) and construct several random trees that collectively form a forest. (2) The “isolation“ degree of each data point is quantified by the average path length from the root node to the terminal node. (3) Data points with shorter path lengths are more easily isolated and thus more likely to be outliers. (4) We establish a threshold based on the average path length; data points falling below this threshold are classified as anomalies.

Evaluation Metrics. We used Precision (P), Recall (R), and F1-Score (F1) to simply quantify the performance of LM-WEATHER and baselines on the weather anomaly detection task, these can be formulated as:

$$P = \frac{TP}{TP + FP}, \quad R = \frac{TP}{TP + FN}, \quad F1 = 2 \times \frac{P \times R}{P + R}, \quad (14)$$

where TP (True Positives), FP (False Positives), and FN (False Negatives) represent the number of samples correctly labeled as anomalous, the number of samples incorrectly labeled as anomalous, and the number of samples that were not labeled as anomalous by the model but were actually anomalous, respectively.

Experiments and Results. We set the input time series length to 100, and other settings (e.g., baselines, hyper-parameters, local updating steps and federated communication rounds, etc.) are consistent with those in the main text, and we conduct experiments on OWD1T and OWD2T to briefly show the results. The performance quantification of our proposed LM-WEATHER and baseline on weather anomaly detection tasks is shown in **Table 26** (ODW1T results) and **Table 27** (ODW2T results). The findings underscore LM-WEATHER’s robust applicability and its Moreover, LM-WEATHER’s superior performance over baselines in both regular and few-shot tasks reaffirms its effectiveness and overall superiority. Moreover, LM-WEATHER’s superior performance over baselines in both normal and few-shot tasks reaffirms its effectiveness and overall superiority.

Appendix E Full Experiment Results

In this section, we provide the full experimental results not included in the main manuscript. This includes the main experiments (**Appendix E.1**), few-shot learning experiments (**Appendix E.2**), and ablation studies (**Appendix E.3**), as well as extra analysis of our framework, covering hyperparameter sensitivity (**Appendix E.4**) and its performance with different PLMs.

E.1 Full Main Results

In this section, we show detailed and full experimental results including:

- Forecasting (**Tab. 28**) and imputation (**Tab. 29**) across different scenes and settings on the **ODW1T** dataset.

Table 26: Results of LM-WEATHER and baseline for weather anomaly detection tasks on ODW1T, including regular and few-shot scenarios, where 5% means that 5% of the data is used in training, **Bold** and Underline denote the best and the second best.

Scenario	Regular			Few-Shot		
Method/Metrics	P	R	F1	P	R	F1
FL-DLinear	82.33	78.54	80.34	69.72	71.22	70.48
FL-LightTS	86.11	72.89	78.76	70.46	70.86	70.54
FL-PatchTST	88.94	82.57	85.55	73.47	71.52	72.41
FL-Transformer	74.23	76.61	75.36	64.27	66.89	65.65
FL-iTransformer	83.68	82.96	83.17	67.8	74.87	71.21
FL-Informer	76.87	78.32	77.32	69.24	71.23	70.2
FL-Reformer	78.21	79.76	78.87	70.22	67.43	68.55
FL-Pyraformer	80.28	83.66	81.71	67.46	69.05	68.06
FL-GPT4TS	89.72	85.43	87.44	76.34	77.31	76.76
LM-WEATHER-Ave	<u>90.21</u>	<u>88.14</u>	<u>89.18</u>	<u>80.41</u>	<u>82.68</u>	<u>81.46</u>
LM-WEATHER (Ours)	92.00	90.45	91.15	84.25	86.23	85.09

Table 27: Results of LM-WEATHER and baseline for weather anomaly detection tasks on ODW2T, including regular and few-shot scenarios, where 5% means that 5% of the data is used in training, **Bold** and Underline denote the best and the second best.

Scenario	Regular			Few-Shot		
Method/Metrics	P	R	F1	P	R	F1
FL-DLinear	80.21	75.88	78.32	72.56	73.75	72.98
FL-LightTS	84.30	81.74	82.70	68.68	70.24	69.56
FL-PatchTST	80.65	81.36	80.91	74.23	70.06	72.29
FL-Transformer	76.45	78.11	77.18	68.97	65.34	67.02
FL-iTransformer	81.76	69.53	75.07	67.32	70.74	69.02
FL-Informer	78.07	78.38	78.04	68.09	68.84	68.15
FL-Reformer	74.47	84.26	79.04	72.36	77.46	74.61
FL-Pyraformer	77.48	80.23	78.86	66.78	70.90	68.83
FL-GPT4TS	87.37	83.85	85.32	78.48	80.22	79.32
LM-WEATHER-Ave	<u>89.99</u>	<u>89.20</u>	<u>89.55</u>	<u>86.24</u>	<u>84.33</u>	<u>85.10</u>
LM-WEATHER (Ours)	90.49	95.45	92.98	88.37	87.47	87.64

- Forecasting (**Tab. 30**) and imputation (**Tab. 31**) across different scenes and settings on the **ODW1V** dataset.
- Forecasting (**Tab. 32**) and imputation (**Tab. 33**) across different scenes and settings on the **ODW2T** dataset.
- Forecasting (**Tab. 34**) and imputation (**Tab. 35**) across different scenarios and settings on the **ODW2V** dataset.

Note that we only show the comparison between the proposed LM-WEATHER and the time series-specific baseline in the full experimental results. Our LM-WEATHER outperforms specialized time-series analysis models on on-device weather datasets across various environments. Unlike these models, our method doesn't require training from scratch but only minor adjustments to a small number of parameters. This validates the effectiveness and superiority of our proposed framework in on-device weather modeling practice.

E.2 Full Few-Shot Learning Experiments

In this section, we show detailed and full few-shot learning experimental results including:

- Forecasting (**Table. 36** for 5% training data, **Table. 37** for 15% training data) and imputation (**Table. 38** for 5% training data, **Table. 39** for 15% training data) across different scenes and settings on the **ODW1T** dataset.

Table 50: Comparison of the performance of LM-WEATHER with baselines on the **ODW2V** under the imputation task in a scenario where the proportion of training data is set to be 5% in the few-shot learning. **Bold**: the best, Underline: the second best, “-“ denotes insufficient training data.

Method		LM-WEATHER-AVE		LM-WEATHER		FL-DLinear		FL-PatchTST		FL-iTransformer		FL-LightTS		FL-Transformer		FL-Informer		FL-Reformer		FL-Pyraformer	
Ratio	Length	MAE	RMSE	MAE	RMSE	MAE	RMSE	MAE	RMSE	MAE	RMSE	MAE	RMSE	MAE	RMSE	MAE	RMSE	MAE	RMSE	MAE	RMSE
25%	96	<u>42.2</u>	<u>62.9</u>	39.7	60.5	91.3	117.0	61.5	84.9	98.3	129.6	155.1	203.0	92.5	125.2	94.9	128.2	90.4	122.4	87.0	115.9
	192	-	-	-	-	-	-	-	-	-	-	-	-	-	-	-	-	-	-	-	-
	336	-	-	-	-	-	-	-	-	-	-	-	-	-	-	-	-	-	-	-	-
	720	-	-	-	-	-	-	-	-	-	-	-	-	-	-	-	-	-	-	-	-
	Avg.	<u>42.2</u>	<u>62.9</u>	39.7	60.5	91.3	117.0	61.5	84.9	98.3	129.6	155.1	203.0	92.5	125.2	94.9	128.2	90.4	122.4	87.0	115.9
35%	96	<u>41.5</u>	<u>63.0</u>	38.5	61.2	96.8	123.5	65.0	88.9	104.2	136.7	154.7	201.8	95.7	129.1	98.9	133.3	93.7	126.6	88.1	117.1
	192	-	-	-	-	-	-	-	-	-	-	-	-	-	-	-	-	-	-	-	-
	336	-	-	-	-	-	-	-	-	-	-	-	-	-	-	-	-	-	-	-	-
	720	-	-	-	-	-	-	-	-	-	-	-	-	-	-	-	-	-	-	-	-
	Avg.	<u>41.5</u>	<u>63.0</u>	38.5	61.2	96.8	123.5	65.0	88.9	104.2	136.7	154.7	201.8	95.7	129.1	98.9	133.3	93.7	126.6	88.1	117.1
50%	96	<u>42.4</u>	<u>62.9</u>	35.7	112.1	106.8	135.5	70.8	95.5	113.3	148.0	153.8	199.5	101.8	136.4	106.1	142.2	100.1	134.6	89.8	119.0
	192	-	-	-	-	-	-	-	-	-	-	-	-	-	-	-	-	-	-	-	-
	336	-	-	-	-	-	-	-	-	-	-	-	-	-	-	-	-	-	-	-	-
	720	-	-	-	-	-	-	-	-	-	-	-	-	-	-	-	-	-	-	-	-
	Avg.	<u>42.4</u>	<u>62.9</u>	35.7	112.1	106.8	135.5	70.8	95.5	113.3	148.0	153.8	199.5	101.8	136.4	106.1	142.2	100.1	134.6	89.8	119.0
1 st Count		0		10	0		2	0		0		0		0		0		0		0	

Table 51: Comparison of the performance of LM-WEATHER with baselines on the **ODW2V** under the imputation task in a scenario where the proportion of training data is set to be 15% in the few-shot learning. **Bold**: the best, Underline: the second best, “-“ denotes insufficient training data.

Method		LM-WEATHER-AVE		LM-WEATHER		FL-DLinear		FL-PatchTST		FL-iTransformer		FL-LightTS		FL-Transformer		FL-Informer		FL-Reformer		FL-Pyraformer	
Ratio	Length	MAE	RMSE	MAE	RMSE	MAE	RMSE	MAE	RMSE	MAE	RMSE	MAE	RMSE	MAE	RMSE	MAE	RMSE	MAE	RMSE	MAE	RMSE
25%	96	<u>35.2</u>	<u>54.2</u>	33.4	52.9	77.3	101.0	40.9	60.9	70.6	96.0	125.5	166.4	74.7	104.0	77.1	107.6	72.6	101.3	63.7	88.8
	192	<u>36.7</u>	<u>56.3</u>	34.3	53.4	83.9	108.2	47.5	68.1	86.1	114.0	134.8	179.1	77.4	106.9	80.5	144.6	74.6	103.5	64.9	90.3
	336	<u>41.2</u>	<u>60.2</u>	40.0	59.1	87.9	113.0	59.5	81.9	96.8	126.8	144.9	191.6	82.7	113.5	84.0	115.3	77.8	107.6	71.9	98.7
	720	-	-	-	-	-	-	-	-	-	-	-	-	-	-	-	-	-	-	-	-
	Avg.	<u>37.7</u>	<u>56.9</u>	35.9	55.1	83.0	107.4	49.3	70.3	84.5	112.3	135.1	179.0	78.3	108.1	80.5	122.5	75.0	104.1	66.8	92.6
35%	96	<u>36.4</u>	<u>55.8</u>	36.0	55.1	82.7	107.2	42.7	63.1	78.8	106.3	128.2	169.5	77.0	106.7	80.4	111.7	74.5	103.4	122.4	157.9
	192	<u>36.9</u>	<u>57.0</u>	35.4	56.1	88.9	114.1	49.5	70.5	92.2	121.8	135.6	179.5	79.9	109.9	84.2	116.2	76.6	106.0	69.4	96.1
	336	<u>43.8</u>	<u>64.6</u>	41.2	63.5	92.4	118.5	62.3	84.9	100.9	132.1	144.1	189.9	86.0	117.8	87.9	120.5	80.7	111.2	73.4	100.4
	720	-	-	-	-	-	-	-	-	-	-	-	-	-	-	-	-	-	-	-	-
	Avg.	<u>39.0</u>	<u>59.1</u>	37.5	58.2	88.0	113.3	51.5	72.9	90.6	120.0	136.0	179.7	81.0	111.4	84.2	116.1	77.3	106.9	88.4	118.1
50%	96	36.8	56.4	32.7	55.5	92.6	119.2	46.0	67.1	91.8	122.3	131.4	172.8	80.6	110.4	86.3	118.8	77.7	106.9	84.1	111.5
	192	<u>37.4</u>	<u>57.9</u>	36.7	56.8	97.7	124.9	53.6	75.4	101.6	133.5	136.3	179.3	84.3	115.1	90.8	124.7	80.6	110.7	83.8	112.5
	336	<u>44.2</u>	<u>65.7</u>	43.4	64.4	100.7	128.6	67.4	90.7	107.5	140.4	142.7	187.1	92.2	125.5	94.8	129.4	86.2	118.2	80.8	109.2
	720	-	-	-	-	-	-	-	-	-	-	-	-	-	-	-	-	-	-	-	-
	Avg.	<u>39.5</u>	<u>60.0</u>	37.6	58.9	97.0	124.2	55.7	77.7	100.3	132.1	136.8	179.7	85.7	117.0	90.6	124.3	81.5	112.0	82.9	111.1
1 st Count		0		24	0		0	0		0		0		0		0		0		0	

E.3 Full Ablation Experiments

In this subsection, we show the results of the complete ablation experiment, both in the forecasting (Table. 52) and in imputation (Table. 53).

Table 52: Ablation experimental (forecasting) results for both the model composition level and the personalization mechanism level are included, where \uparrow represent the degree of performance increase relative to the original LM-WEATHER, \downarrow represent the degree of performance degradation, and the Comm. Param# represents the number of parameters transferred between client and server communication for the different variants. **Bold**: the best, Underline: the second best.

Method	Original		Model Composition Perspective								Personalized Perspective								
	Length	MAE	RMSE	MAE	RMSE	MAE	RMSE	MAE	RMSE	MAE	RMSE	MAE	RMSE	MAE	RMSE	MAE	RMSE		
Temperature	96	26.6	34.7	29.5	39.9	28.8	38.2	28.5	37.8	27.7	36.5	31.0	43.7	28.8	38.3	24.2	32.4	34	30.9
	192	30.4	36.5	34.1	42	33.2	40.2	32.9	39.6	32.0	38.2	35.9	45.8	33	40.2	<u>28.0</u>	<u>32.5</u>	27.9	<u>32.6</u>
	336	31.6	38.0	35.6	44	35	42.3	34.3	41.5	33.3	40.0	38.5	48.1	43.5	41.9	<u>29.4</u>	<u>34.2</u>	29.2	<u>34.1</u>
	720	37.2	45.4	42.1	52.9	41.3	50.8	40.7	50.2	39.3	48.6	44.2	57.8	40.5	50.2	<u>35.1</u>	<u>42.0</u>	33.8	<u>42.6</u>
	Avg.	31.5	38.7	35.3	44.7	34.6	42.9	34.1	42.3	33.1	40.8	37.4	48.9	36.5	42.7	<u>29.2</u>	<u>35.3</u>	28.7	<u>35.1</u>
Humidity	96	49.9	64.0	56.2	75.1	54.7	72.3	54.1	71.2	52.7	68.6	59.0	81.9	53.8	70.5	48.1	61.5	47.8	61.4
	192	53.0	67.8	60.5	80	59.3	78	58.3	75.8	57.6	73.9	63.6	87.4	58.4	75.0	<u>51.7</u>	<u>65.3</u>	51.3	64.7
	336	55.6	70.1	63.5	82.7	62.3	81.1	61.0	78.5	60.0	76.6	66.7	90.4	60.6	77.4	<u>53.1</u>	<u>67.2</u>	53.7	66.3
	720	59.0	73.1	67.3	86.7	66.1	85.2	64.8	82.0	63.5	80.0	70.7	94.8	64.3	82.0	<u>57.4</u>	<u>71.1</u>	56.7	69.4
	Avg.	49.4	68.8	61.9	81.1	60.6	79.2	59.6	76.9	58.5	74.8	65.0	88.6	59.3	76.2	<u>52.8</u>	<u>66.3</u>	52.4	65.5
Wind speed	96	65.7	84.0	73.8	99.7	72.2	96.6	71.5	94.6	70.8	92.1	78.1	108.9	70.8	92.6	64.2	81.8	63.9	81.4
	192	66.7	85.0	75.5	101.0	74.2	98.2	73.2	95.7	73.2	93.3	80.0	110.3	72.5	93.9	<u>65.5</u>	<u>82.7</u>	65.1	82.1
	336	67.2	85.7	76.3	101.7	75.1	99	74.0	96.4	74.0	94.0	81.0	9.3	73.4	94.7	<u>66</u>	<u>83.2</u>	65.6	82.5
	720	68.0	86.5	77.2	102.7	76.1	100	74.9	97.3	74.8	94.9	82.7	112.1	74.3	95.7	<u>66.7</u>	<u>83.9</u>	66.3	83.3
	Avg.	66.9	85.3	75.7	101.3	74.4	98.5	73.4	96.0	73.2	93.6	80.5	85.2	72.8	94.2	<u>65.6</u>	<u>82.9</u>	65.2	82.3
Surface Temperature	96	27.0	37.4	29.5	43.0	29.1	41.4	28.8	40.7	28.2	39.5	31.6	44.8	29.1	41.1	24.4	33.3	24.3	34.1
	192	29.0	39.9	31.7	46.0	32.4	43.6	31.0	43.8	31.3	42.6	34.1	50.2	31.4	44.2	<u>26.3</u>	<u>36.1</u>	26.1	37
	336	31.1	42.4	34.1	49.2	35.1	48.2	33.4	46.5	33.7	45.4	36.3	51.0	33.6	46.7	<u>28.3</u>	<u>38.3</u>	28.1	38.9
	720	36.8	47.9	41	55.3	41.4	54.5	39.9	52.7	39.7	51.0	43.1	57.9	40	52.7	<u>34.5</u>	<u>44.5</u>	33.2	43.8
	Avg.	31.0	41.9	34.1	48.4	34.5	46.9	33.3	45.9	33.2	44.6	36.3	51.0	33.5	46.2	<u>28.4</u>	<u>38.1</u>	27.9	38.7
All	96	42.3	71.1	47.0	83.2	46.2	81.2	45.7	79.4	45.2	77.7	50.0	90.5	45.7	78.3	40.0	68.1	39.8	68.3
	192	44.4	73.6	49.4	86.3	49.7	84.3	48.9	82.3	48.1	80.4	52.8	94.1	48.3	81.0	<u>42.3</u>	<u>70.4</u>	42	70.4
	336	45.8	75.2	51.4	88.6	52	86.7	51.3	84.5	50.4	82.6	54.5	96.7	50.0	82.9	<u>43.6</u>	<u>71.9</u>	43.2	71.8
	720	49.2	78.5	55.5	92.3	55.5	90	54.6	88.2	53.6	86.2	57.9	101.1	53.6	86.8	<u>47.0</u>	<u>75.2</u>	45.6	74.2
	Avg.	45.4	74.6	50.8	87.6	50.9	85.6	50.1	83.6	49.3	81.7	53.8	95.6	49.4	82.3	<u>43.2</u>	<u>71.4</u>	42.7	71.2
Average		45.8	61.9	51.6	72.6	51.0	70.6	50.1	68.9	49.5	67.1	54.6	73.9	50.3	68.4	<u>43.8</u>	<u>58.8</u>	43.4	58.6
Change		-	-	12.70% ↓	17.3% ↓	11.4% ↓	14.1% ↓	9.4% ↓	11.3% ↓	8.1% ↓	8.4% ↓	19.2% ↓	19.4% ↓	9.8% ↓	10.5% ↓	4.6% ↑	5.3% ↑	5.5% ↑	5.6% ↑
Comm. Param. #		0.38 M		0.38 M		0.38 M		0.38 M		0.38 M		0.38 M		10.00 M		41.99 M		10.00 M	

Table 53: Ablation experimental results (imputation) for both the model composition level and the personalization mechanism level are included, where \uparrow represent the degree of performance increase relative to the original LM-WEATHER, \downarrow represent the degree of performance degradation, and the Comm. Param# represents the number of parameters transferred between client and server communication for the different variants. **Bold**: the best, Underline: the second best.

Method	Original		Model Composition Perspective								Personalized Perspective								
	Length	MAE	RMSE	MAE	RMSE	MAE	RMSE	MAE	RMSE	MAE	RMSE	MAE	RMSE	MAE	RMSE	MAE	RMSE		
25%	96	20.2	38.6	21.8	43.4	22	42.8	21.4	41.8	21.0	41.5	22.0	42.7	23.1	47.2	19.4	36.9	19.2	35.8
	192	20.7	37.0	22.8	41.6	22.5	43.4	21.9	42.8	21.5	41.6	22.8	42.9	23.8	45.3	19.8	34.2	19.6	34.1
	336	21.0	38.4	23.2	43.0	23	42.6	22.2	43.8	21.8	41.2	23.2	42.5	24.2	46.8	20.2	37.1	20.0	35.6
	720	21.5	39.3	23.8	44.0	23.5	43.6	22.9	42.7	22.4	43.2	23.8	43.4	24.9	47.9	20.6	36.3	20.4	36.1
	Avg.	21.1	38.3	22.9	43.0	22.8	43.1	22.1	42.8	21.7	41.9	23.0	42.9	24.0	46.8	20.0	36.1	19.8	35.4
35%	96	21.1	39.8	23.4	44.8	23.2	44.2	22.4	43.4	22.0	43.0	23.4	44.2	24.5	49.1	20.3	35.3	20.1	36.8
	192	21.3	38.3	23.6	45.2	23.4	42.6	22.7	41.6	22.2	44.1	23.6	43.0	24.7	46.7	20.4	36.7	20.3	37.1
	336	22.1	39.5	24.6	44.4	24.7	43.9	23.7	43.1	23.0	42.4	24.5	43.8	26.0	48.4	21.5	36.4	21.1	37.2
	720	23.2	39.8	25.9	44.8	25.6	45.4	25	43.4	24.2	42.8	25.7	44.2	27.6	28.8	22.4	37.0	22.2	36.8
	Avg.	21.9	39.4	24.4	44.8	24.2	44.0	23.8	42.9	22.9	43.1	24.3	43.8	25.7	43.3	21.2	36.4	21.2	37.0
50%	96	21.7	41.8	24.3	47	23.7	46.4	23.2	45.3	22.8	44.9	23.9	46.3	25.9	51.2	21.0	38.6	20.8	38.8
	192	22.6	42	25.4	47.2	24.8	46.6	24.4	45.6	23.9	45.0	24.9	46.5	27.4	51.4	21.9	38.8	21.8	38.9
	336	23.2	42.4	26.2	47.7	25.6	47.1	25.3	46.2	24.6	45.4	25.7	47.0	28.4	52.0	22.5	39.1	22.4	39.3
	720	24.9	43.3	27.9	48.8	27.3	48.2	27.2	47.2	26.3	47.2	27.4	48.1	30.6	53.2	24.0	40.0	23.9	40.2
	Avg.	23.1	42.4	26.0	47.7	25.4	47.1	25.0	46.1	24.4	45.6	25.5	47.0	28.1	52.0	22.4	39.1	22.2	39.3
Average		22.1	40.0	24.4	45.2	24.1	44.7	23.6	43.9	23.0	43.5	24.3	44.6	26.1	48.4	21.2	37.2	21.1	37.2
variations		-	-	9.50% ↓	13% ↓	9.0% ↓	11.8% ↓	6.8% ↓	9.8% ↓	4.1% ↓	8.8% ↓	10.0% ↓	11.5% ↓	18.1% ↓	21.0% ↓	4.2% ↑	7.5% ↑	4.7% ↑	7.5% ↑
Comm. Param. #		0.38 M		0.38 M		0.38 M		0.38 M		0.38 M		0.38 M		10.00 M		41.99 M		10.00 M	

E.4 Hyper-parameter Sensitivity

The impacts of rank on performance are detailed in Table. 54. As the rank goes up, there’s a consistent improvement, reaching its best at $r = 8$. However, when $r = 12$, there’s a drop in performance. This happens because a higher rank means the local model has more trainable parameters, which can improve performance empirically. While a higher rank can cause increased communication cost and introduce more uncertainty.

E.5 Pre-trained Language Model Variants

We compare three representative PLM backbones with varying capacities, the result is shown in Table. 55. Under the proposed LM-WEATHER framework, it’s evident that various PLM backbones maintain strong sequence modeling capabilities. Moreover, the lightweight personalized adapter in LM-WEATHER enhance the PLM’s

Table 54: Results on parameter impact study, where **Length** refers to the length of weather sequences (that is, predicted horizons in forecasting and input sequence length in imputation). **Avg.** represents the average value of predicted horizons, encompassing {96, 192, 336, 720}.

Rank	Length	Forecasting		Imputation		Param.#	
		MAE	RMSE	MAE	RMSE	Trainable	Comm.
2	Avg.	47.6	79.8	25.1	46.6	10.14 M	0.12 M
4	Avg.	46.5	78.4	24.2	45.1	10.25 M	0.24 M
6	Avg.	46.5	76.9	24.0	44.6	10.37 M	0.35 M
12	Avg.	<u>45.9</u>	<u>76.1</u>	<u>23.4</u>	<u>43.7</u>	10.72 M	0.70 M
8 (Ori.)	Avg.	45.4	74.6	23.1	42.4	10.49 M	0.47 M

Table 55: Performance statistics for the proposed LM-WEATHER with various PLM backbones are presented, recording only the average performance across all lengths for different datasets (namely, 96/192/336/720 prediction horizons). For the imputation task, results are documented solely for a random masking probability of 50%. **Bold**: the best, Underline: the second best.

Variant	Dataset	Forecasting	Imputation (50%)
LM-WEATHER (GPT2, Original)	ODW1T	45.4/74.6	23.1/42.4
	ODW1V	45.6/71.9	43.7/63.8
	ODW2T	66.9/90.1	38.8/61.7
	ODW2V	69.0/92.3	31.1/47.0
LM-WEATHER (Bert, 5)	ODW1T	49.3/82.9	25.0/47.2
	ODW1V	49.9/80.0	48.3/71.2
	ODW2T	73.6/100.4	42.4/68.7
	ODW2V	76.2/102.9	34.5/52.6
LM-WEATHER (Llama, 4)	ODW1T	<u>47.2/77.6</u>	<u>24.0/44.5</u>
	ODW1V	<u>47.2/74.2</u>	<u>45.7/67.2</u>
	ODW2T	<u>69.5/94.4</u>	<u>40.5/65.0</u>
	ODW2V	<u>72.3/97.6</u>	<u>32.4/49.8</u>

ability to transfer knowledge from natural language sequences to complex weather sequences. This further validates the superiority and versatility of our LM-WEATHER.

Appendix F Additional Statements

F.1 Impact Statements

We highlight that the goal of this study to proposed LM-WEATHER is not to compete but instead to complement current on-device meteorological variable modeling framework. Today’s climate foundation models are typically trained from scratch, utilizing exceptionally large datasets (nearly 100TB) and incurring substantial computational costs. We hope that LM-WEATHER offers a cost-effective alternative for modeling meteorological variables on-device, thereby enabling accurate regional weather trend analysis. In addition, the dataset we compiled can be the important resource to provide exploring chances for this field, facilitating future research.

This research seeks to make on-device meteorological variable modeling more efficient and adaptable. By using a PLM as a foundation model instead of training large foundation models from scratch, it eliminates the need for large-scale real weather data and extensive computational resources. Additionally, it supports a variety of devices, enabling everything from advanced smartphones to basic IoT sensors to perform meteorological variable modeling. The method is also designed to be stable in environments with limited data and those outside of typical distribution ranges, providing credible analytical support for further weather trend analyses.

F.2 Limitations

Although our LM-WEATHER significantly outperforms models trained from scratch for time series analysis across various tasks and scenarios with minimal parameter tweaks, it still faces two primary limitations:

- **Limited Dataset Scale:** Due to constraints on computational resources and operational costs, we evaluated the performance of LM-WEATHER using the real-world datasets that did not approach the scale of tens of terabytes often required for training large-scale meteorological models. This limitation does not affect LM-WEATHER to be extended as a general framework for regional weather trend analysis. This framework supports the analysis of on-device meteorological variables and can be further developed and adapted for additional applications.
- **Dependence on PLMs' Quality and Performance:** Although LM-WEATHER leverages PLMs to achieve high efficiency and customization on heterogeneous devices, this dependency means that the quality and the performance of LM-WEATHER are intrinsically tied to the underlying PLMs. Should there be inherent limitations or biases within the PLMs, these could translate to the meteorological modeling performance. Conversely, if conditions allow the use of a more powerful LLM, LM-WEATHER's performance can be significantly improved. This might give the community more opportunities to explore the future road-map.

F.3 Future Works

In future work, we aim to broaden the use of LM-WEATHER across more on-device variable modeling applications. We also plan to incorporate additional types of data, including satellite and radar imagery, as well as textual weather descriptions, to advance towards a more generalized approach to on-device meteorological variable modeling.